MODULATION OF P53 SIGNALING IN an APT$_{121}$ INDUCED PROSTATE CANCER MODEL

Wenqi Pan

A dissertation submitted to the faculty of the University of North Carolina at Chapel Hill in partial fulfillment of the requirements for the degree of Doctor of Philosophy in the Curriculum of Genetics and Molecular Biology.

Chapel Hill
2011

Approved by

Advisor: Yanping Zhang

Reader: Beverly H. Koller

Reader: Adrienne D. Cox

Reader: Norman E. Sharpless

Reader: Jean Cook

ABSTRACT

Wenqi Pan: Modulation of p53 signaling in an APT$_{121}$ induced prostate cancer model
(Under the Direction of Dr. Yanping Zhang)

Recently, an APT$_{121}$-induced prostate cancer mouse model was generated, in which Rb and its family members, p107 and p130, are inhibited, therefore leading to initiation and progression of prostate cancer. In the APT121 prostate cancer model, germline deletion of p53 has been shown to accelerate epithelial tumors as well as stromal tumors induced by paracrine stress signals from epithelial cells. However, given that human cancer is often the result of a somatic mutation rather than a germline mutation, the model described above cannot fully mimic the human situation. To address this issue, we have generated a mouse model harboring a somatic deletion of p53 in prostate epithelial cells. Through the development of a pre-clinical mouse model that more closely recapitulates the human disease, we are able to further explore the function of p53 signaling in response to Rb inhibition. Moreover, to investigate the potential therapeutic effects of p53 on prostate cancer, we utilized a p53 knock-in mouse model, p53^{ER}, in which inactive p53 can be restored to its active state by tamoxifen treatment. Our study shows that

somatic deletion of p53 accelerates tumor progression and confirms that the stromal tumors observed in the previous report are indeed caused by paracrine signaling from epithelial cells.

In the second part of our study, we focused on novel p53 signaling which has been reported to play a critical role in maintaining cell homeostasis after ribosomal stress. Disruption of the binding of ribosomal proteins (RP) and Mdm2 (a primary inhibitor of p53) in the Mdm2 point-mutation mouse model $Mdm2^{C305F}$, has been shown to attenuate p53 signaling in Myc-induced lymphoma. This suggests that RP-Mdm2-p53 signaling could be a general tumor suppressor pathway activated in response to a variety of oncogenic stresses. To investigate this possibility, we crossed $Mdm2^{C305F}$ mice with APT_{121} mice. Our results showed that disruption of the RP-Mdm2-p53 pathway does not accelerate prostate tumorigenesis induced by APT_{121}. Instead, the p19Arf-Mdm2-p53 pathway is the major player in response to Rb inhibition.

All these studies have revealed the importance of p53 in the APT_{121} mouse model of prostate cancer.

To all those I love and those love me,

Your trust and support made me who I am.

TABLE OF CONTENTS

List of Tables

Table

List of Figures

Figure

List of Abbreviations

1. **ARR2PB**   compostite probasin promoter

2. **CDK**   cyclin dependent kinase

3. **CP**   cytoplasm

4. **H&E**   hematoxylin-eosin

5. **IHC**   immunohistochemistry

6. **KO**   knock out

7. **LOH**   loss of heterozygosity

8. **NO**   nucleolus

9. **NP**   nucleoplasm

10. **PB**   rat small probasin promoter

11. **RP**   ribosomal protein

12. **SV40**   simian virus 40

13. **T_{121}**   a truncated T-Ag comprised of the N-terminal 121 amino acids

14. **TRAMP**   Transgenic Adenocarcinoma of the Mouse Prostate

15. **TUNEL**   terminal deoxynucleotidyl transferase mediated dUTP nick end labeling

16. **WT**   wild-type

CHAPTER ONE

INTRODUCTION

Prostate Cancer in Humans

Prostate cancer is the second leading cause of cancer death in American men, behind only lung cancer. According to the American Cancer Society, about 217,730 new cases of prostate cancer were diagnosed in the United States in 2010, and 32,050 men died of prostate cancer. About 1 man in 6 will be diagnosed with prostate cancer during his lifetime (American cancer society: Cancer facts and figures 2010). Although the majority of patients initially respond well to androgen ablation, eventually nearly all men with advanced prostate cancer progress to hormone-refractory prostate cancer (HRPC). At this stage, chemotherapy may be used to extend survival, yet no curable therapeutic option is available (1). Despite the magnitude of the statistics, the underlying causes of prostate cancer remain elusive mainly due to the heterogeneity of genetic alterations found in the tumors (2). Several tumor suppressor genes have been implicated including Rb (Retinoblastoma) (3) and p53 (also known as protein 53 or tumor protein 53) (4).

APT$_{121}$ Mouse Model of Prostate Cancer

Rb and its family members p107, and p130 control the G1 to S-phase transition of the cell cycle primarily by interacting with the E2F family of transcription factors(5). Rb recruits chromatin-remodeling proteins, such as histone deactylases and histone methyl-transferases to repress the transcriptional activation of E2F1 (6-8). It was reported that 27% of human prostatic adenocarcinomas lost one RB allele (9) and both reduced expression of Rb mRNA and pRb protein have been reported (10-11).

Mice lacking the Rb gene die at around 13 days of gestation before the prostate forms (12). Mice heterozygous for Rb or chimeric for Rb develop only pituitary or thyroid tumors (13-15). Somatic deletion of Rb in mouse epithelial cells only leads to early stage of prostate cancer (16). This appears to be because of compensation by p107 and/or p130 in many murine cell types (17).

To bypass the redundancy of p107 and p130 in mice while focusing on the function of the pRb family alone in the development of prostate cancer, the *APT$_{121}$* prostate cancer mouse model was generated by Dr. Terry Van Dyke's lab. *APT$_{121}$* is a truncated SV40 large T antigen (maintains the first $_{121}$ NH2-terminal amino acids; *T$_{121}$*) under the probasin promoter. The transgene binds Rb and its family members, p130 and p107, and is specifically expressed in prostate epithelium (Figure 1A). When Rb is suppressed, E2F1 is activated and cells become tumorigenic. As early as 8 weeks of age, the prostates of *APT$_{121}$* mice exhibit dysplasia. *APT$_{121}$* mice show mouse prostatic intraepithelial neoplasia (mPIN) by 12 weeks old, characterized by tufting epithelial layers that form cribriform patterns. The prostates of *APT$_{121}$*

develop micro-invasive adenocarcinomas by 16 weeks old, characterized as epithelial cells

breaking through the basement membrane into the stroma (Figure 1B) (18)

When APT_{121} mice are crossed with $p53^{-/-}$ mice, stromal tumors, identified as the

presence and introductal growth patterns of stromal cells (Figure 2A and 2B), were greatly

accelerated by p53 haploinefficiency.   Stromal tumors occur as early as 5 months old in

$APT_{121};p53^{+/-}$ mice. In contrast, stromal tumors occur only randomly and much later in

$APT_{121};p53^{+/+}$ mice (Figure 2A) (18).

Figure 1. **APT$_{121}$ mouse prostate cancer model** (18)**.**

A. A diagram of APT$_{121}$ mouse model: a truncated SV40 large T antigen under probasin promoter. The expression of the transgene is targeted to mouse prostate epithelial cells. The transgene is studied in the B6D2F1 mouse.

B. Histological pictures demonstrated the progression of tumors in *APT$_{121}$* mice at 2 months (Dysplasia), 3 months (mPIN) and 4 months (Adenocarcinoma) of age.

A

wt SV40
T Ag

pRb

p53
inactivation

ARR2Pb

pRB$_f$

pRb, p107, p130
Inactivation in the
prostate epithelial cells

Strain: B6D2F1
A cross between female
C57BL/6 and male DBA/2.

ARR2PbT121 = APT121

B

Wild Type

APT$_{121}$

2 Months   30μm

2 Months

3 Months

Normal

Single cell layer

Dysplasia

-Epithelial cell tufting
-Increase in proliferation
-Appearance of
apoptotic bodies

mPIN

-Cribriform architecture
-Presence of rounded
nuclei

micro-invasive
adenocarcinoma

4 Months

Figure 2. Progression of epithelial tumor and stromal tumor in APT$_{121}$;p53$^{-/-}$ mice (18).

A. A diagram of p53 status and tumor progression in APT$_{121}$ mice. p53 heterozygousity does not affect the onset of epithelial tumors, yet it accelerates the onset of stromal tumors with tumors appearing in mice by 5 month of age. *APT$_{121}$;p53$^{+/-}$* mice die around 7 months due to the enlargement of tumors. Both epithelial and stromal tumors are greatly advanced in *APT$_{121}$;p53$^{-/-}$* mice and mice die around 5 months of age.

B. Large tumors in *APT$_{121}$;p53$^{-/-}$* mice are comprised of extensive stromal component. Star indicates the stromal regions of tumors.

A

B

APT$_{121}$;p53$^{-/-}$

50μM
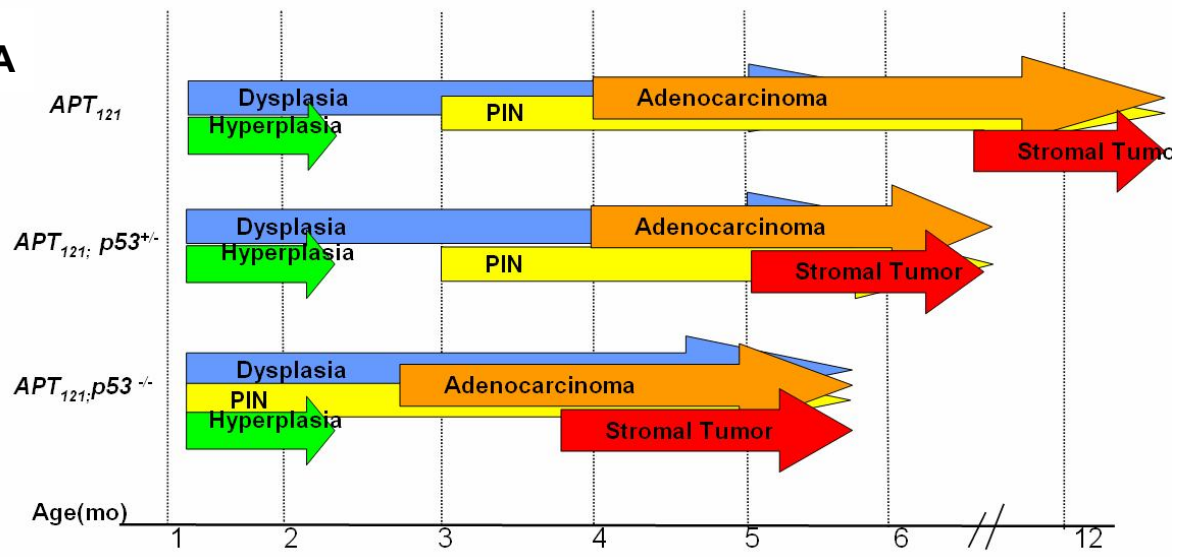
p53^{ER} Mouse Model

p53^{ER} mice were generated by Gerard Evan lab (19). The hormone-binding domain of the modified estrogen receptor, ER^{TAM} (20) was fused to p53 at the its' 3'-end (Figure 3A). In the absence of 4-hydroxytamoxifen, p53$^{m/m}$ mice are similar to p53 null mice. Both develop tumors of the similar incidence and spectrum, though the onset of tumors in the p53$^{ER/ER}$ mice was slightly delayed (Figure 3B).

Figure 3. A diagram of the p53ER^m allele (19)

The ligand binding domain of estrogen receptor is fused to the 3' end of p53 allele. Without

tamoxifen, p53 is inactive. With tamoxifen, p53 is active.

p53^{ER} allele
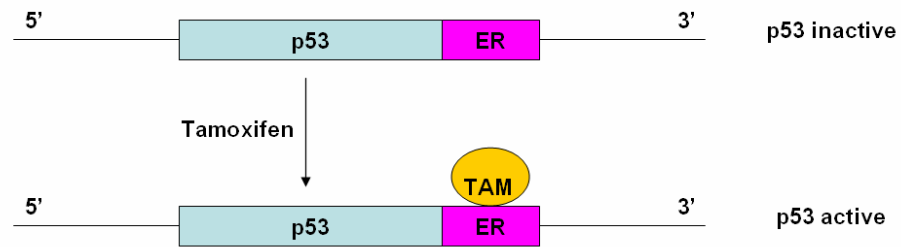
Without tamoxifen injection, *APT121;p53* $^{ER/-}$ *= APT121;p53* $^{-/-}$

With tamoxifen injection, *APT121;p53* $^{ER/-}$ *= APT121;p53* $^{+/-}$

RP-Mdm2-p53 Signaling Pathway

p53 is well known as the guardian of the genome. Under stress such as DNA damage, oncogenic stress and hypoxia, p53 is stabilized and activated, resulting in the induction of a variety of downstream signaling pathways, including cell cycle arrest, apoptosis, DNA repair and senescence (21). Under normal condition, the level of p53 is kept low mainly by its inhibitor, Mdm2 (mouse double minute 2). The C-terminus of Mdm2 has an intrinsic E3 ligase activity which promotes the ubiquitiation and degradation of p53. The N-terminus of Mdm2 binds to the transactivation domain of p53 and inhibits the recruitment of co-activators. Additionally, Mdm2 is directly transactivated by p53, thereby forming an Mdm2-p53 feedback loop to maintain cellular homeostasis (22). p53 has been found to be mutated in about 50% of human tumors, indicative of its importance in tumorigenesis (23). In addition to mutation of p53 directly, overexpression of Mdm2 can also cause tumors (24).

The ribosome is the 'factory' for protein synthesis. The mammalian 80S ribosome is comprised of a large 60S and a small 40S ribosomal subunit. The 60S large subunit contains 5S, 5.8S, and 28S rRNAs and around 47 large ribosomal proteins (RPL). The 40S small subunit contains 18S rRNA and around 32 small ribosomal proteins (RPS). Ribosomal subunits are made in the nucleolus and exported to the cytoplasm for the assembly of ribosomes. Ribosomal biogenesis requires balanced expression between rRNAs and ribosomal proteins, processing of rRNA precursors into mature rRNAs and assembly of 40S and 60S ribosomal subunits into 80S ribosome (25). When any of these steps are disrupted, for instance, via drug-treatment with mycophenolic acid (MPA) (26), actinomycin D (Act D)(27)

or 5-fluorouracil (5-FU) (28), ribosomal stress is induced. In addition to drug treatment, changing cell culture conditions, such as serum starvation and contact inhibition(29), or overexpression of nucleostemin or the dominant negative mutant Bop1(30) can also induce ribosomal stress.

Under ribosomal stress, free forms of RPs (RPL and RPS), including L11 (31-32), L23 (33-34) , and L5 (27), S7 (35) enter the nucleoplasm to interact with the zinc finger domain of Mdm2. This binding by L11, L23 or L5 inhibits MDM2's E3 ligase function, resulting in p53 accumulation and activation (Figure 4). Knockdown of L11 and L5 does not induce a p53 response, whereas knockdown of L23 does induce a p53 response. This indicates that these ribosomal proteins function similarly as well as distinctly to transmit ribosomal stress to the Mdm2-p53 pathway.

S7 forms a ternary complex with Mdm2 and p53. Mdm2 can target S7 for ubiquitination, and MdmX (homolog of Mdm2) enhances the inhibition of Mdm2 by S7 (36). L26 also binds the zinc finger domain of mdm2 and besides that, L26 binds to the 5′ untranslated region (UTR) of p53 mRNA and augments its translation. The binding between Mdm2 and L26 promotes the ubiquitination and degradation of L26 and therefore, weakens p53 augmentation by L26 (37).

Figure 4. Diagram of RP-Mdm2-p53 signaling (38).

Under normal conditions, large and small ribosomal subunits are assembled in the nucleolus (NO) and then exported to the cytoplasm (CP) for protein synthesis. However, under nucleolar stress, the balance between rRNA and ribosomal proteins (RPL and RPS) is disrupted. Free forms of ribosomal proteins are released from the NO to the nucleoplasm (NP) and bind to Mdm2. p53 is thereby activated and stabilized. Excess free forms of ribosomal proteins can also be released from cytoplasmic ribosomes and then enter the NP, interacting with Mdm2.

14
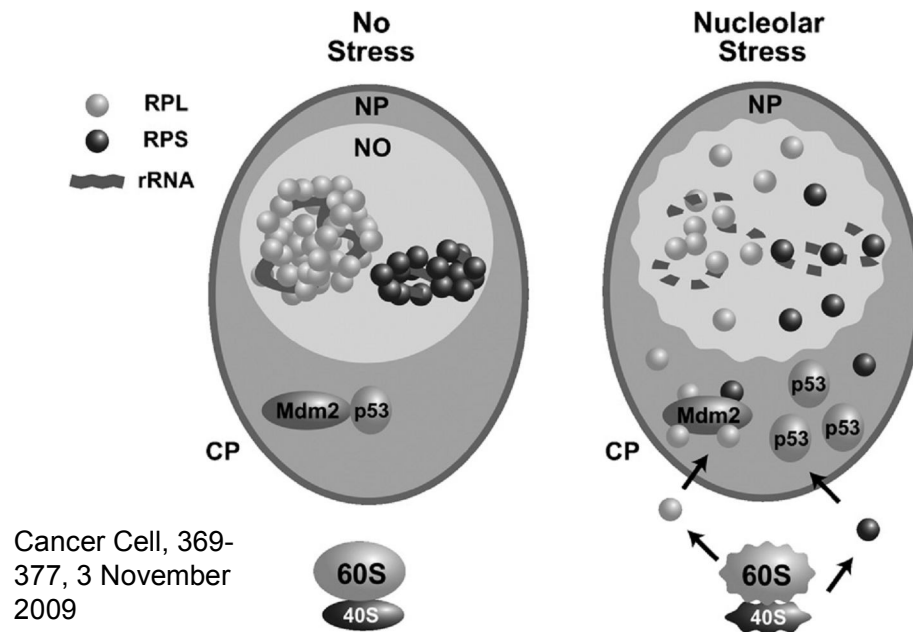
Mdm2^C305F Knock-in Mouse Model

In vitro data have shown that mutation of the zinc-coordinating cysteine (C) residues to phenylalanine (F) disrupts Mdm2's interaction with L11 and L5 while retaining interaction with L23 (Figure 5). As a result, The $MDM2^{C305F}$ mutant is attenuated in mediating p53 degradation after ribosomal stress (39). Based on in vitro data, our lab generated the $Mdm2^{C305F/C305F}$ knock-in mouse (40). And the characterization of $Mdm2^{C305F}$ knock-in mouse and Eu-Myc study are also done by a former lab member, Dr. Everardo Macias.

Figure 5. A diagram showing that a point mutation of Mdm2 disrupts its binding to ribosomal proteins L11 and L5 (40)
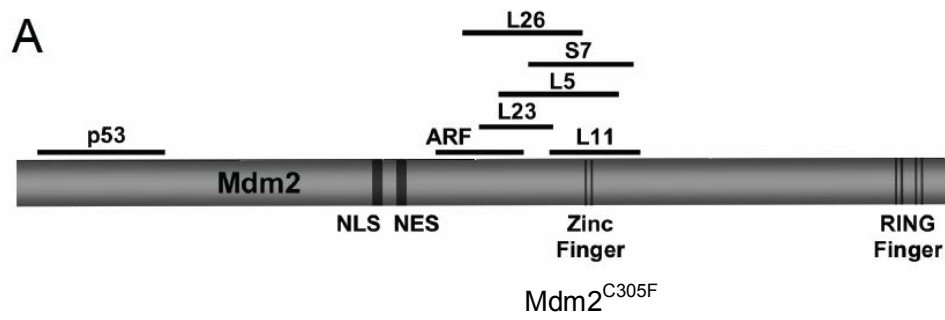
The Mdm2^{C305F} mutation disrupts L5 and L11 binding (40)

Previous study also investigated the binding activity of the *Mdm2^{C305F}* mutant protein.

Mouse embryonic fibroblasts (MEFs) were used for an immunoprecipitation-coupled western

blot (IP-western) assay (40). When cell lystates were immunoprecipitated with anti-Mdm2

antibody and then immunoblotted with anti-L5 and anti-L11 antibody, L5 and L11 were

present in the *Mdm2^{+/+}* but not in the *Mdm2^{C305F/C305F}* immunoprecipitates (Figure 7A).

Mdm2^{C305F} was still able to bind p53.   Because the anti-Mdm2 antibody (clone 2A10) affects

the binding between Mdm2 and L23, we cannot evaluate the interaction of L23 with Mdm2

using immunoprecipitation. We can however immunoprecipitate with anti-L23 antibody and

then detect Mdm2 by western blotting. As shown in Figure 7B, L23 still binds to *Mdm2^{C305F}*.

The result is consistent with previous in vitro studies (39).

Figure 6.   Mdm2^{C305F} mutant protein does not bind to L11 and L5 (40)

A. *Mdm2$^{+/+}$* and *Mdm2$^{m/m}$* MEFs were treated with 5 nM Act D. Cell lysates were

immunoprecipitated with anti-*Mdm2* antibody and to detect Mdm2, p53, L5 and L11 as

indicated. 5% of total IP lysate is used as loading control.

B. MEFs were treated as in (A), and cell lysates were analyzed as indicated.
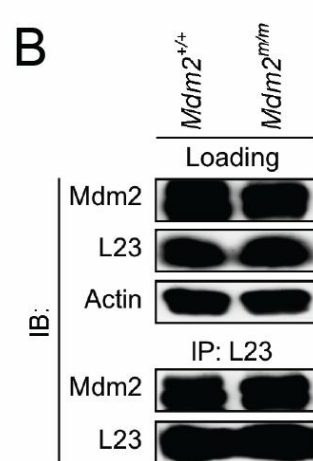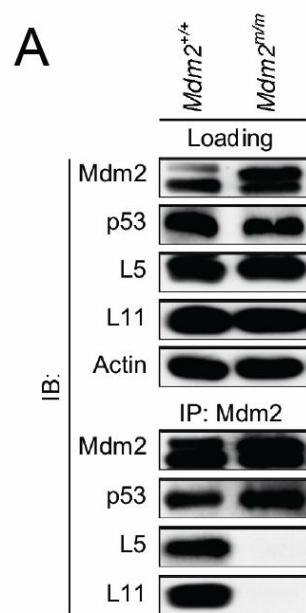
Mdm2^{C305F} mutation attenuates p53 response to ribosome biogenesis stress (40)

Ribosomal stress induces releasing free forms of PRs, such as L11 and L5. L11 and L5 can bind to Mdm2 and thereby, leads to p53 stabilization and activation. Since the *Mdm2^{C305F}* mutant protein cannot bind to L5 and L11 as shown in figure 6, it is expected that the p53 response would be attenuated after ribosomal stress. To assess this, *Mdm2$^{+/+}$, Mdm2$^{+/C305F}$*, and *Mdm2$^{C305F/C305F}$* MEFs were either untreated or treated with a low dose of actinomycin D (5nM Act D). *Mdm2$^{+/+}$* MEFs exhibited the highest induction of p53, compared to *Mdm2$^{+/C305F}$* showing intermediate induction of p53, and *Mdm2$^{C305F/C305F}$* with the lowest induction of p53 (Figure 9A). Two other drug, 5-FU and MPA, are also known to induce ribosomal stress. MEF cells were treated with these two drugs to further confirm that p53 induction was attenuated in *Mdm2$^{C305F/C305F}$* MEFs. Figure 9B show that again the p53 response is attenuated in a gene dosage dependent manner. Taken together, the data show that the p53 response to ribosomal stress is attenuated in *Mdm2^{C305F}* MEFs (40).

Figure 7. *Mdm2^{C305F}* **MEFs exhibit attenuated p53 response to ribosome biogenesis stress** (40)**.**

A. MEFs were either mock treated or treated with 5 nM Act D for 12 hr and then harvested for western blotting analysis.

B. MEFs were treated with 1 µM 5-FU or 2 µM MPA for 12 hr and examined for p53 protein level by western blotting.

A

Control   Act D 5nM

Mdm2: +/+ +/m m/m +/+ +/m m/m

p53

Actin

B

5-FU   MPA

Mdm2: +/+ +/m m/m   +/+ +/m m/m

p53

Actin
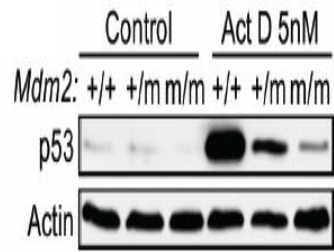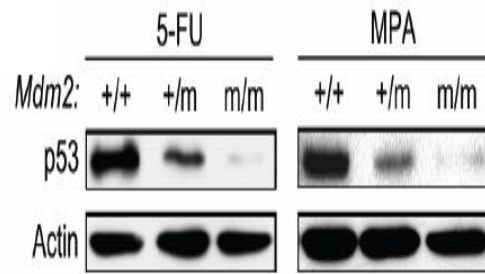
Myc-induced lymphomagenesis is accelerated by Mdm2^{C305F} mutation (40)

Translocation (t8;14) of Myc into or close to Ig loci is often observed in Burkitt's B cell lymphoma (41). To mimic this in the mouse model, the Myc gene was coupled to an Emu immunoglobulin heavy chain enhancer, resulting in the overexpression of Myc in the B cell lineage (42). Eμ-myc mice die of B cell lymphoma and the median survival is 20 weeks. The Eμ-*Myc;Mdm2$^{+/C305F}$* mice had a median survival of about 15 weeks, while the survival of Eμ-*Myc;Mdm2$^{C305F/C305F}$* mice was reduced to a median of 9 weeks (Figure 10A). Tumors from the Eμ-*Myc;Mdm2$^{C305F/C305F}$* mice were morphologically similar to those from Eμ-*Myc;Mdm2$^{+/+}$* mice (Figure 10B) (40). Given that Myc upregulates ribosomal biogenesis by interacting with all three RNA polymerases (43), these findings established the RP-Mdm2-p53 signaling as a genuine barrier against Myc-induced tumors.

Figure 8. Myc-induced lymphomagenesis is accelerated by Mdm2^{C305F} mutation (40) .

A. Survival of Eμ-*Myc* transgenic mice. Eμ-*Myc;Mdm2*$^{+/+}$ (+/+, n = 24), Eμ-*Myc;Mdm2*$^{+/m}$ (+/m,

n = 27), and Eμ-*Myc;Mdm2*$^{m/m}$ ($^{m/m}$, n = 18) mice.

B. Graph shows the lymphomas in a 58-day old Eμ-*Myc;Mdm2*$^{m/m}$ mice.

A

B *Eμ-myc;Mdm2^{m/m}*
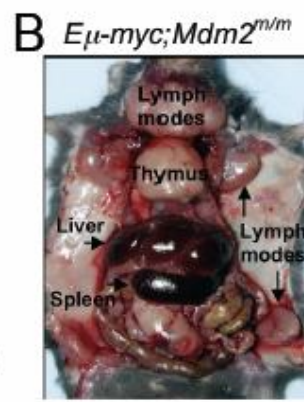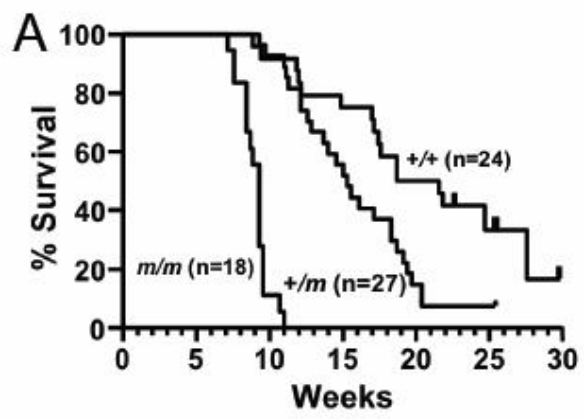
RP-Mdm2-p53 functions in a pattern similar to p19Arf-Mdm2-p53 in response to Myc

Eµ–*myc* transgenics that were wild-type for *p19Arf* displayed a mean survival of 20 weeks (42), while Eµ–*myc* transgenics heterozygous for *p19Arf* displayed a mean survival of 11 weeks. Eµ–*myc*;*p19Arf* ^{−/−} mice die soon after birth in some offspring, and of those that survived initially, all died of lymphoma by 8 weeks of age (44)(Figure 8A). Tumors from Eµ–*myc*;*p19Arf* ^{−/−} mice were phenotypically indistinguishable from those from wild-type Eµ–*myc* transgenics. Noticeably, this pattern of tumor acceleration is very similar to the accelerated tumorigenesis observed in mice harboring the *Mdm2*^{C305} mutation in the Eµ–*myc* background (40)(Figure 8B).

Figure 9. Myc-induced tumorigenesis is accelerated by loss of *ARF* (44).

Survival of Eμ-*Myc* transgenic mice. Eμ-*Myc; ARF*$^{+/+}$ (ARF+/+, n = 31), Eμ-*Myc; ARF*$^{+/-}$

(*ARF*$^{+/-}$, n = 85), and Eμ-*Myc; ARF*$^{-/-}$ (*ARF*$^{-/-}$, n = 20) mice. Lymphoma was documented in

all the animals.

ARF+/+ (n=31)

ARF+/- (n=85)

ARF-/-
(n=20)

% Survival

Weeks

28
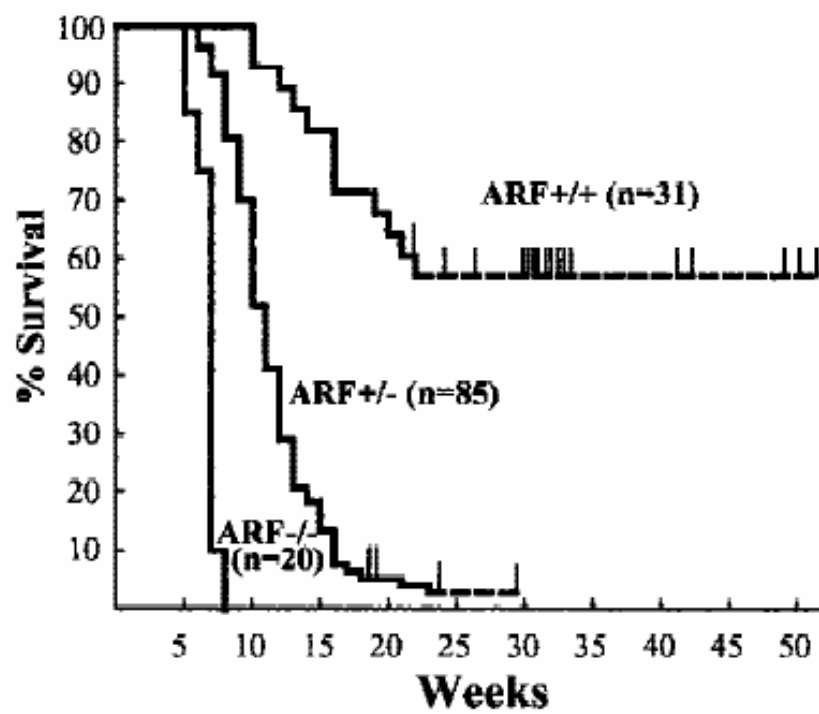
CHAPTER TWO

Targeted p53 deletion in APT_{121}-initiated epithelial cells accelerates prostate cancer development that can be reversed by p53 restoration

Abstract

In the *APT_{121}* mouse model, Rb and its family members, p107 and p130, are inactivated specifically in prostate epithelial cells by expression of APT_{121}, an SV40 T antigen N-terminal fragment placed under regulation of the prostate epithelium-specific probasin promoter. It has been shown that *APT_{121}* transgenic mice develop prostatic intraepithelial neoplasia (mPIN), which further progresses into adenocarcinomas, and that this phenotype is accelerated by additional germline mutation of p53. However, prostate cancer is a disease more commonly associated with somatic mutations. Thus, we sought to investigate the role of somatic p53 deletion in the development of prostate epithelial tumors. Here, we generated *$APT_{121};p53^{cf/f}$;Pb-Cre* mice, in which the expression of APT_{121} and deletion of p53 occur simultaneously and specifically in the prostate of compound male mice at 6 weeks of age, as a preclinical animal model to both genetically and biologically emulate human prostate cancer. We show that deletion of p53 significantly accelerated prostate adenocarcinoma formation as well as the development of stromal tumors through a

mechanism that favors cell proliferation without affecting apoptosis. In addition, we took advantage of the previously generated $p53^{ER}$ mouse model where tamoxifen treatment re-establishes wild-type p53 function and developed $APT_{121};p53^{ER/-}$ mice to evaluate the consequence of restoration of p53 in prostate cancer cells. We show that reinstating p53 function by treating $APT_{121};p53^{ER/-}$ mice with tamoxifen resulted in decreased proliferation and increased apoptosis in the prostate, and significantly reduced tumor progression. Together, our data suggest that p53 plays a crucial role in prostate cancer initiation and progression and that therapies focusing on restoring p53 activity in epithelial cells could be an attractive approach to not only prevent malignant progression but also to delay the onset of prostate stromal tumors.

Acknowledgement

Introduction

Prostate cancer is the second most common cancer among men. 25 to 50% of human

prostate adenocarcinomas harbor aberrations in the Retinoblastoma (Rb) pathway. Rb is a

tumor suppressor that binds to and represses the transcriptional activity of E2F family

transcription factors that control the G1-S cell cycle transition. Phosphorylation of Rb by

Cdk4/6-Cyclin D or Cdk2-Cyclin E releases Rb from the E2F complex, allowing

transactivation of E2F target genes to occur. Rb inactivation is common in prostate cancer

and generally precedes somatic alterations affecting the tumor suppressor gene p53 (45).

Functional interactions between the two major tumor suppressor genes appear to directly

influence tumor development in the mouse prostate (46). In particular, mutations of the p53

gene are frequently associated with metastasis and an androgen depletion–independent

phenotype in prostate cancer (47).

Targeted inactivation of p53 in a murine model of prostate cancer was found to induce

mouse Prostatic Intraepithelial Neoplasia (mPIN) but failed to progress to invasive carcinoma,

indicating that loss of p53 may be a synergistic rather than an initiative event in promoting

prostate tumorigenesis (48). On the other hand, deletion of both the *Rb* and *p53* genes in

mice resulted in rapid development of invasive and metastatic prostate cancer (49). Further

studies indicated that the cell origin of prostate cancer associated with p53 and Rb deficiency

is likely to be stem/progenitor cells that control luminal and neuroendocrine differentiation

(50).

The *APT$_{121}$;p53$^{+/-}$* and *APT$_{121}$;p53$^{-/-}$* mouse models revealed that these animals

experienced a great susceptibility to the development of oversized tumors comprised of

adenocarcinomas and a large amount of abnormal stromal hyperproliferation (18, 51).

However, germline mutation in the *p53* gene does not seem to be an early event in prostate

tumorigenesis; rather, it seems to be associated with the development of malignant

progression. Thus, we proposed to investigate whether somatic inactivation of *p53* in the

prostate epithelium of *APT$_{121}$* mice alters the onset of adenocarcinomas and whether it

participates in the development of stromal tumors.

Results

Prostate epithelial-specific deletion of p53 accelerates adenocarcinoma development and induces stromal tumors in APT_{121}-induced prostate cancer

Prostate cancer is mostly associated with somatic gene mutations rather than germline gene mutations. In this context, results obtained from various mouse models have shown that complete ablation of *p53* in mice may influence tumor development by altering the cell microenvironment. Thus, we sought to provide a preclinical system that could better simulate the human disease by generating a mouse model with prostate-specific somatic deletion of *p53*. We generated APT_{121} compound mice carrying a probasin-driven Cre/loxP system (52) to obtain conditional ablation of p53 expression. We bred the previously developed $p53^{cf/f}$ conditional knockout mice (53) with Probasin-Cre transgenic mice (Pb-Cre) (48), which express the Cre transgene in the epithelial cells of the prostate beginning at the onset of puberty around 6 weeks of age. The $p53^{cf/f}$;*Pb-Cre* mice were then crossed with APT_{121} mice to generate APT_{121};$p53^{cf/f}$;*Pb-Cre* compound mice. Thus, expression of APT_{121} and deletion of *p53* occur simultaneously and in the same cellular compartment in the compound mice at 6 weeks of age.

We established tumor appearance by harvesting prostates from wild type, $APT_{121,}$ *and* APT_{121};$p53^{cf/f}$;*Pb-Cre* mice every four weeks beginning at 8 weeks of age. To evaluate tumor progression, hematoxylin and eosin staining (H&E) of tissue sections was used. All groups of mice were monitored daily for signs of morbidity and prostate cancer development. None of the wild type littermates developed neoplasias during the course of these studies (Table 1).

However, consistent with previous reports (18), the APT_{121} mice developed mPIN at 12 weeks (75% incidence), which further transformed into adenocarcinomas by 4 months of age (75% incidence) (Table 1). The APT_{121};$p53^{cf/f}$;Pb-Cre mice displayed a shorter latency for tumor development as reflected by the appearance of mPIN at 8 weeks with a 66% incidence. At 3 months, APT_{121};$p53^{cf/f}$;Pb-Cre mice had already developed adenocarcinomas with an 87.5% incidence, and by 5 months we observed 100% incidence of stromal neoplasias, consistent with a previous study of the APT_{121}; $p53^{-/-}$ mouse prostate model (51). Interestingly, in the presence of wild type p53 APT_{121} prostates did not show stromal tumors until later in life, after 11 months, and with a low incidence (30%) (Table 1). The survival rate correlated with the malignancy and progression of the tumors, as all of the APT_{121};$p53^{cf/f}$;Pb-Cre mice died or had to be sacrificed by 5-6 months due to the tumor burden (Table 1 and Figure 10B). This phenotype was not apparent in mice harboring wild-type p53 (APT_{121} and WT mice) (Table 1 and Figure 10A). H&E staining of wild type prostates from 5-month old animals exhibited normal prostate acini architecture arranged in a lobular configuration, consisting of a single layer of luminal cells and a layer of epithelial cells surrounded by a basement membrane separating the prostate gland from the stroma. The stroma, in turn, is formed by two to three layers of smooth muscle with loose connective tissue found between the glands (Figure 10C). APT_{121} prostates showed adenocarcinomas with the classic "acinar type" phenotype in which the tumor is thought to arise from or recapitulate prostatic acini (Figure 10D). The acinar type is characterized by back-to-back proliferation of small- to intermediate-sized tumor acini with scant to moderate intervening stroma. No stromal tumors were detected in APT_{121} prostates

at this age. In contrast, the $APT_{121};p53^{cf/f};Pb\text{-}Cre$ compound mice displayed

poorly-differentiated adenocarcinomas with infiltration of the prostate acina into the

fibromuscular stroma and multiple areas where the basal cell layer was absent, highlighting

the invasive and malignant nature of these tumors (Figure 10E). Furthermore, the enlarged

tumors were comprised of a large portion of stromal neoplastic cells that expanded into the

glands (Figure 10F).

Altogether, these data indicate that deletion of $p53$ in the epithelium of APT_{121} prostates

results in early tumor onset with features of malignancy, invasion, and the occurrence of

stromal neoplasia, the latter of which is likely induced by a paracrine effect from the abnormal

epithelial cells to the surrounding mesenchymal tissue. This is consistent with the hypothesis

that in $APT_{121};p53^{+/-}$ prostates, the oncogenic stress in prostate epithelium signals a

mitogenic stimulation to the mesenchyme leading to the development of stromal tumors (51).

It is of note that prostatic stromal tumors have also been found in humans (54-56).

Table 1. Early onset of prostate cancer in *APT$_{121}$; p53$^{cf/f}$; Pb-Cre* mice

Genotype	mPIN	Adenocarcinoma	Stromal tumor	Survival
Wild-type	None (0/4)	None (0/5)	None (0/5)	>18 months
APT$_{121}$	3 months (3/4)	4 months (6/8)	>11 months (3/10)	>15 months
APT$_{121}$; p53$^{cf/f}$; Pb-Cre	2 months (4/6)	3 months (7/8)	5 months (9/9)	5-6 months

Figure 10. Deletion of p53 in prostate epithelium accelerates both adenocarcinoma and stromal tumors in *APT$_{121}$* mice.

Gross anatomy of prostates from *APT$_{121}$* (A) and *APT$_{121}$;p53$^{cf/f}$; Pb-Cre* (B) prostate gland and associated seminal vesicles.. *APT$_{121}$; p53$^{cf/f}$; Pb-Cre* prostate displays solid tumors, dramatically enlarged with important vasculature. Hematoxilin and Eosin (H&E) staining of wild-type prostate (C) shows normal gland architectures.and the inset illustrates the single layer of epithelial cells in the gland. (D) *APT$_{121}$* prostate shows well-differentiated adenocarcinoma, and the inset points out to the intact basement membrane. (E) *APT$_{121}$;p53$^{cf/f}$; Pb-Cre* prostate displays poorly-differentiated adenocarcinoma. The arrow indicates the increased proliferation and loss of basement membrane that resulted in invasion to the stroma. (F) A representative stromal tumor found in *APT$_{121}$;p53$^{cf/f}$; Pb-Cre* prostate, the (*) demarks the stromal neoplasia and the inset shows the expansion of stromal cells inside of the epithelial gland and the lack of organization of the mesenchymal cells. All histological analysis was done in mice of 5 month old.
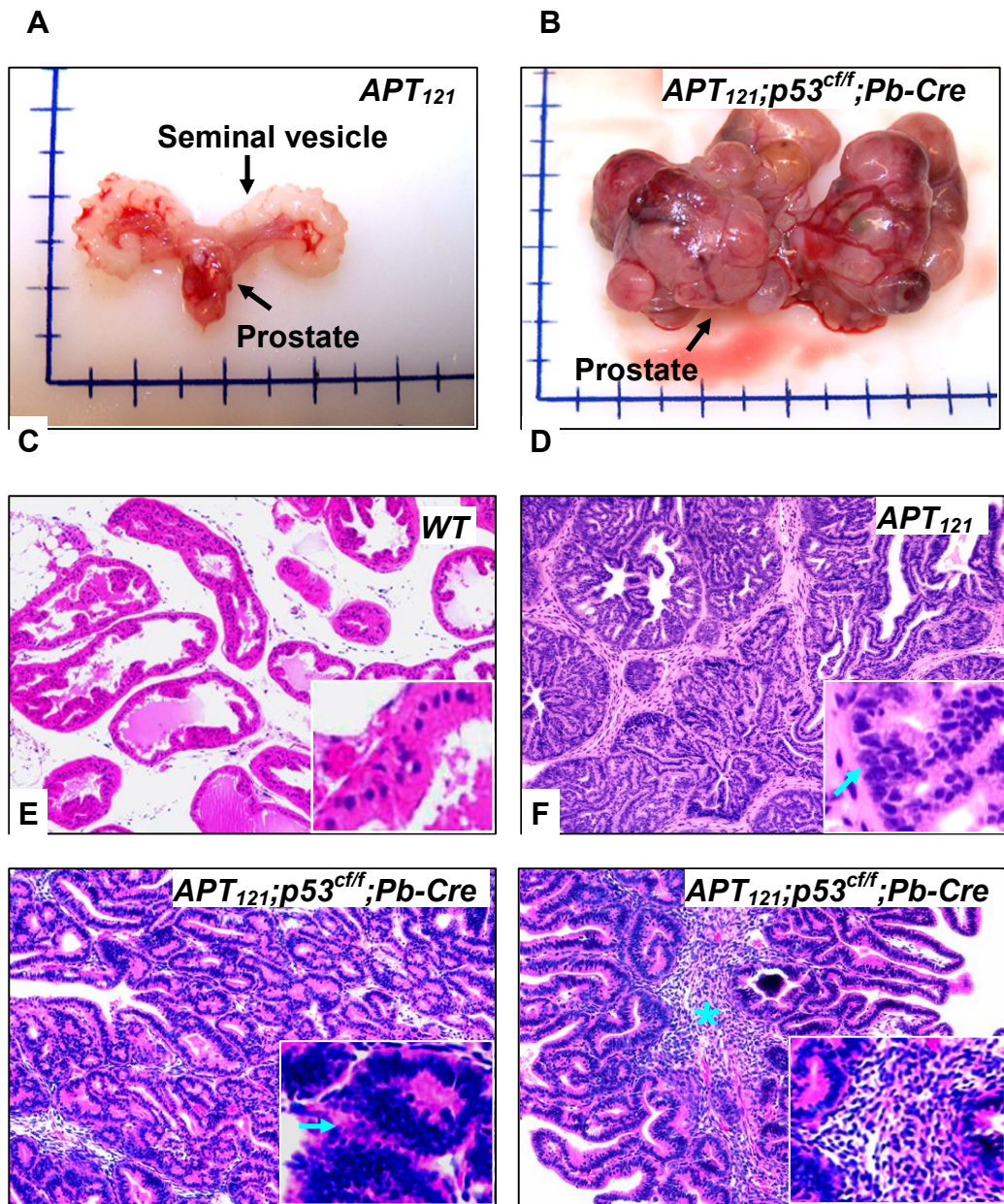
Adenocarcinomas developed in *APT$_{121}$;p53$^{cf/f}$;Pb-Cre* compound mice are not derived from neuroendocrine cells

Some prostate cancer mouse models develop tumors classified as adenocarcinomas, while other models form neuroendocrine carcinomas. It has been previously demonstrated that in some mouse models of prostate cancer, the origin of the tumor and the progression of the disease are influenced by the mouse strain background. One example is the widely used transgenic adenocarcinoma mouse prostate (TRAMP) model. While TRAMP mice with a C57BL/6J background develop adenocarcinomas, TRAMP mice with an FVB background have a significantly shorter lifespan than TRAMP-C57BL/6J mice due to the rapid progression of neuroendocrine carcinomas forming from bipotential progenitor cells at early stages of prostate tumorigenesis(57). Consistent with these studies, the *APT$_{121}$;p53$^{cf/f}$;Pb-Cre* mice, which have a genetic background similar to that of the FVB-TRAMP mice, have a shorter lifespan due to the size and the malignancy of the prostate tumors. We performed a series of immunohistochemistry (IHC) stainings to define the *APT$_{121}$;p53$^{cf/f}$;Pb-Cre* prostate tumor cell origin. We first confirmed that the transgene T$_{121}$ expression was confined to the epithelial compartment (Figure 11A), ruling out the possibility of leaky expression of the transgene. IHC staining showed that the *APT$_{121}$;p53$^{cf/f}$;Pb-Cre* neoplasias were positive for the androgen-receptor (AR), which is a marker expressed in both prostate epithelial and mesenchymal connective cells but not in neuroendocrine cells (Figure 11B). Figure 11C shows that cytokeratin18/8, a marker restricted to luminal epithelial cells, was confined to the

epithelium of prostate tumors, as expected. Lastly, synaptophysin (SYN), a specific marker

for neuroendocrine cells, was negative in all samples tested (Figure 11D), thus ruling out the

possibility that the tumors detected in $APT_{121};p53^{cf/f};Pb\text{-}Cre$ prostates were of neuroendocrine

origin as was reported for the FVB-TRAMP model (57). Together, these evidences indicate

that the tumors formed in $APT_{121};p53^{cf/f};Pb\text{-}Cre$ mice can be classified as adenocarcinomas.

Additionally, we assessed the invasive capacity of the adenocarcinomas by staining for

α-smooth actin (SMA), a marker found at the fibromuscular stromal cell layer that surrounds

the tumors. We observed a loss of this marker at a large portion of the area surrounding the

$APT_{121};p53^{cf/f};Pb\text{-}Cre$ tumors, indicating that the stromal layer was disrupted in this area,

enhancing the tumors' ability to migrate (Figure 11E and 11F). This loss of α-smooth actin

highlights the invasive nature of the $APT_{121};p53^{cf/f};Pb\text{-}Cre$ tumors.

Figure 11. *APT_{121}; $p53^{cf/f}$; Pb-Cre* **cancer cells do not derive from neuroendocrine cells.**

(A) T_{121} IHC staining: Using the SV40 T antigen mouse mAb, the expression of T_{121} is restricted to the prostate epithelial cells of *APT_{121}; $p53^{cf/f}$; Pb-Cre* mice. (B) The Androgen-receptor (AR) IHC staining illustrates that the expression of this marker in the glandular epithelium and the stroma is conserved. (C) Immunofluorescence for cytokeratins 18/8 (CK18/8) shows adequate distribution of luminal epithelia cells. (D) Synaptophysin (SYN) specifically identifies neuroendocrine cells, which were not detected in any of the compound mice tumors. (E) α-smooth actin (SMA) is a marker of fibromuscular cells and underlies the basement membrane of the glandular tissue. (F) As demarked by the arrow and the pointed line, the fibromusular cells distribution becomes lose with areas of complete absence of the expression of this marker, indicating the micro-invasive nature of these tumors.
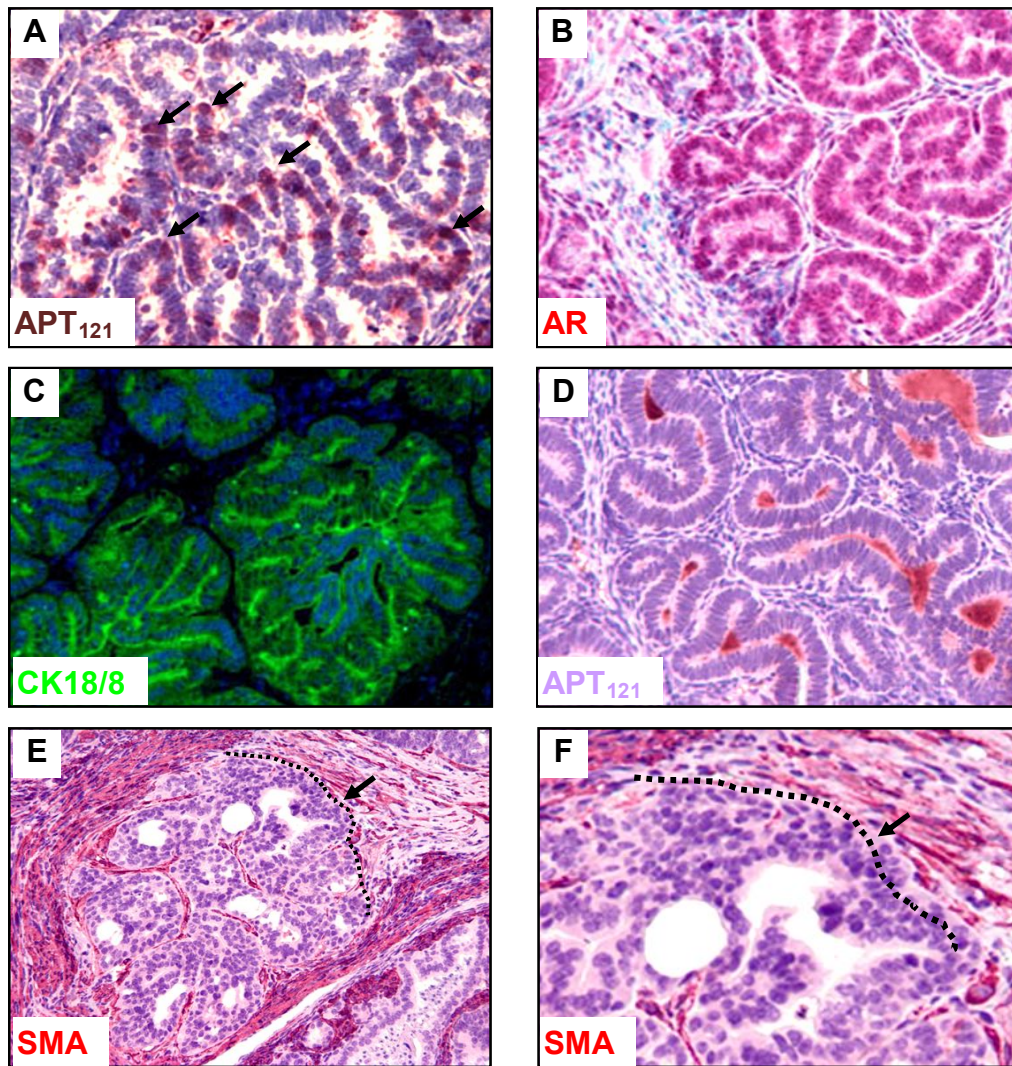
Prostate epithelial-specific deletion of p53 does not affect apoptosis but enhances

proliferation in *APT$_{121}$*-induced prostate cancer

The data presented here demonstrate that specific deletion of *p53* in prostate epithelial

cells results in reduced tumor latency and increased malignancy. In order to understand the

probable mechanism leading to increased tumor growth in *APT$_{121}$;p53$^{cf/f}$;Pb-Cre* prostate

neoplasms, we quantified the rates of proliferation and apoptosis by immunohistochemical

staining. In *APT$_{121}$* prostates, the quantity of proliferating epithelial cells was 49%, as

measured by Ki67 staining (a marker of cell proliferation) (Figure 12A and 12C). The

APT$_{121}$;p53$^{cf/f}$;Pb-Cre prostate epithelial cells were significantly more proliferative than the

APT$_{121}$ cells, with 73% of cells staining positive for Ki67 (Figure 12B and 12C). To measure

the rate of apoptosis in the prostate tumor cells, a TUNEL assay (terminal deoxynucleotidyl

transferase–mediated dUTP-biotin nick end labeling) was used. No significant difference in

apoptosis was observed between *APT$_{121}$;p53$^{cf/f}$;Pb-Cre* prostates and *APT$_{121}$* prostates

(14.2% and 12.2% apoptotic cells, respectively), (Figure 12D-F). These data indicate that

p53 function in the prostate epithelial tissue is important in the regulation of cell proliferation

but is not required for modulation of apoptosis.

Figure 12. p53 deletion in *ATP$_{121}$* prostate induced adenocarcinomas are the results of

increased proliferation but not apoptosis.

(A-B)   Representative Ki67 staining from 5 month-old mice of the indicated genotype. Brown

staining indicates proliferating cells. (C) Average % proliferating cells (Ki67-positive) ± SEM

from 5 month-old mice of the indicated genotype. n=5 for each genotype. At least five

independent fields consisting of a total of at least 1,000 cells from each prostate sample were

counted. *p < 0.05 as assessed by Student's t test. (D-E) Representative TUNEL assay from

5 month-old mice of the indicated genotype. Apoptotic cells are stained purple. (F)   Average

% apoptotic cells (TUNEL-positive) ± SEM from 5 month-old mice of the indicated genotype.

n=5 for each genotype. At least five independent fields consisting of a total of at least 1,000

cells from each prostate sample were counted.

A — *APT₁₂₁* — Ki67
B — *APT₁₂₁;p53^{cf/f};Pb-Cre* — Ki67

C

% Proliferating cells

*p<0.05

APT_{121} $APT_{121};p53^{cf/f};Pb\text{-}Cre$

D — *APT₁₂₁* — TUNEL
E — *APT₁₂₁;p53^{cf/f};Pb-Cre* — TUNEL

F

% Apoptotic cells

p=0.24

APT_{121} $APT_{121};p53^{cf/f};Pb\text{-}Cre$
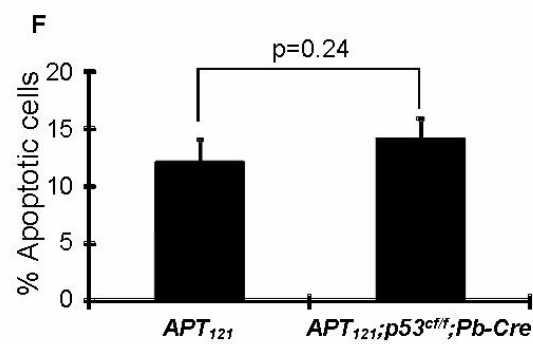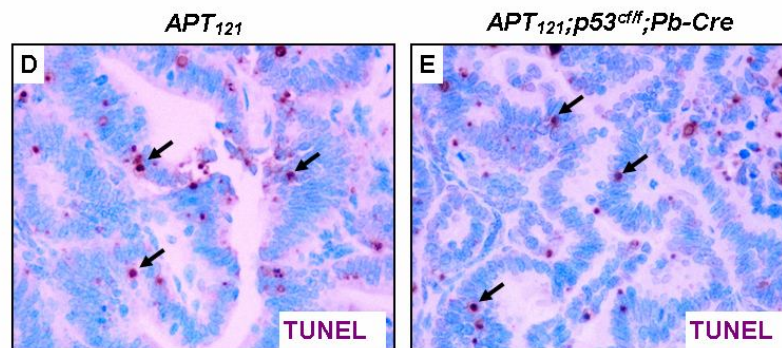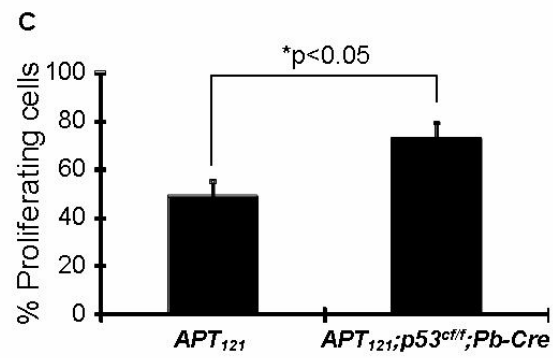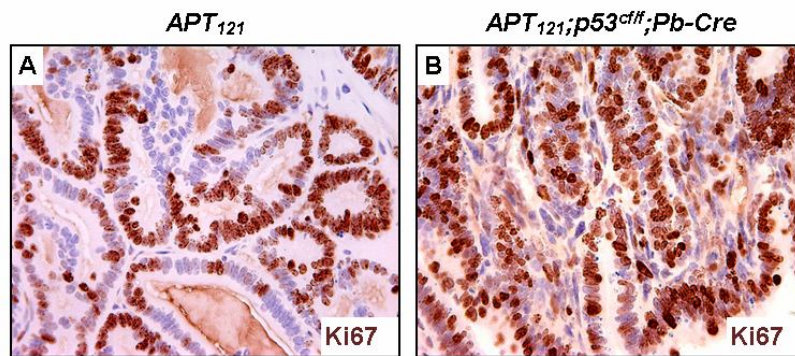
Restoration of p53 function in *APT$_{121}$; p53$^{ER/-}$* mice delays the onset of *APT$_{121}$*-induced prostate cancer by reducing proliferation and increasing apoptosis

We have demonstrated that p53 plays a pivotal role in tumor progression of *APT$_{121}$*-induced prostate cancer. To further investigate the function of p53 in tumor suppression, we took advantage of an inducible-p53 mouse model, *p53^{ER}* (19). These mice have inactive p53 in the absence of tamoxifen, and upon inoculation with this drug, the activity of wild-type p53 is reinstated. We generated and selected *APT$_{121}$;p53$^{ER/-}$* males to evaluate whether the malignant tumor phenotype could be reversed or delayed by restoring p53 function. Without tamoxifen injection, *APT$_{121}$;p53$^{ER/-}$* mice resemble *APT$_{121}$;p53$^{-/-}$* mice. After tamoxifen injection, the *APT$_{121}$;p53$^{ER/-}$* prostate epithelial cells become heterozygous for p53 (*APT$_{121}$;p53$^{+/-}$*). Considering that *APT$_{121}$;p53$^{ER/-}$* mice die around 4 months of age due to oversized prostate tumors, we began tamoxifen treatments at 2 months. Tamoxifen or oil (mock treatment) were introduced intraperitoneally (i.p) every 3 days during a 30-day period (a total of 10 applications). The mice were euthanized within 3 days after the last treatment. Prostate samples were formalin-fixed and paraffin-embedded for histological examination. As shown in Table 2, oil-injected *APT$_{121}$;p53$^{ER/-}$* mice exhibited a 100% incidence of adenocarcinomas. In contrast, the tamoxifen-injected *APT$_{121}$;p53$^{ER/-}$* mice exhibited a dramatic drop in the incidence of adenocarcinomas; instead, the majority of these mice (4 out of 6) showed only mPIN (Table 2). Notably, all *APT$_{121}$;p53$^{-/-}$* mice developed adenocarcinomas (measured at the same time), regardless of tamoxifen treatment. Histochemically, the oil-injected *APT$_{121}$;p53$^{ER/-}$* mice showed clear development of prostate

46

adenocarcinoma, whereas the tamoxifen-treated $APT_{121};p53^{ER/-}$ mice displayed benign,

well-differentiated mPIN (Figure 13A and 13B). The control $APT_{121};p53^{-/-}$ mice displayed, as

expected, prostate adenocarcinoma with all treatments (Figure 13C and 13D). To examine

how reinstating p53 expression in the prostate cells affects tumor onset, prostate sections

were assessed by immunohistochemistry for the expression of Ki67, a proliferation marker,

and with a TUNEL assay. Restoration of p53 expression by tamoxifen injection resulted in a

significant decrease in proliferation and increase in apoptosis in the prostate of $APT_{121};p53^{ER/-}$

mice: Proliferating cells decreased from 44% to 28% of total cells, and apoptotic cells

increased from 8% to 18% (Figure 4M and 4N, open bars). This effect was not observed in

control $APT_{121};p53^{-/-}$ mice (Figure 4M and 4N, filled bars). Representative IHC images were

shown in Figure 13E-H for Ki67 staining and in Figure 13I-L for TUNEL staining. In summary,

our results indicate that the expression of wild-type p53 is essential for preventing malignant

initiation and progression in prostate tumors, and that restoration of p53 function in these

tumor cells can effectively reverse malignant prostate adenocarcinoma progression and

abolish stromal tumor formation.

Figure 13. Restoration of p53 expression in $APT_{121;}$ $p53^{ER/-}$ epithelial cells prevents prostate malignant progression

Representative H&E staining of prostate sections from mice of the indicated genotypes and treatments. (A) $APT_{121;}$ $p53^{ER/-}$ prostate shows adenocarcinomas upon Oil injection. $APT_{121;}$ $p53^{ER/-}$ prostate shows mPIN upon tamoxifen inoculation that results in restoration of p53 expression (B). Both oil-injected and tamoxifen-injected $APT_{121;}$ $p53^{-/-}$ prostates show adenocarcinoma with stromal tumor phenotype.(C and D). Representative Ki67 staining from mice of the indicated treatment. Brown staining indicates proliferating prostatic cells.of oil or tamoxifen-treated $APT_{121;}$ $p53^{ER/-}$ prostates (E and F) and that of oil or tamoxifen-treated $APT_{121;}$ $p53^{-/-}$ prostates (G and H). Representative TUNEL staining from mice of the indicated treatment. Purple staining indicates apoptotic cells of oil or tamoxifen-treated $APT_{121;}$ $p53^{ER/-}$ prostates (I and J) and that of oil or tamoxifen-treated $APT_{121;}$ $p53^{-/-}$ prostates (K and L).

(M) Average % Ki67-positive cells ± SEM from mice of the indicated treatment. n=5-6 for each genotype. At least five independent fields consisting of a total of at least 1,000 cells from each prostate sample were counted. **$p < 0.01$ as assessed by Student's t test. (N) Average % TUNEL-positive cells ± SEM from mice of the indicated treatment. n=5-6 for each genotype. At least five independent fields consisting of a total of at least 1,000 cells from each prostate sample were counted. **$p < 0.01$ as assessed by Student's t test.
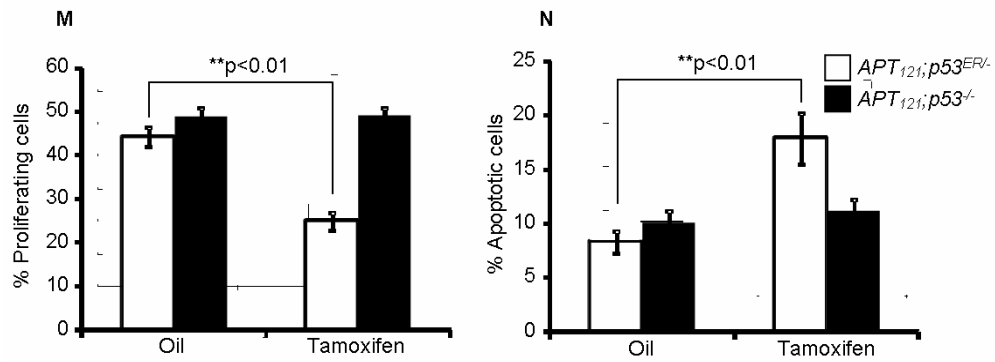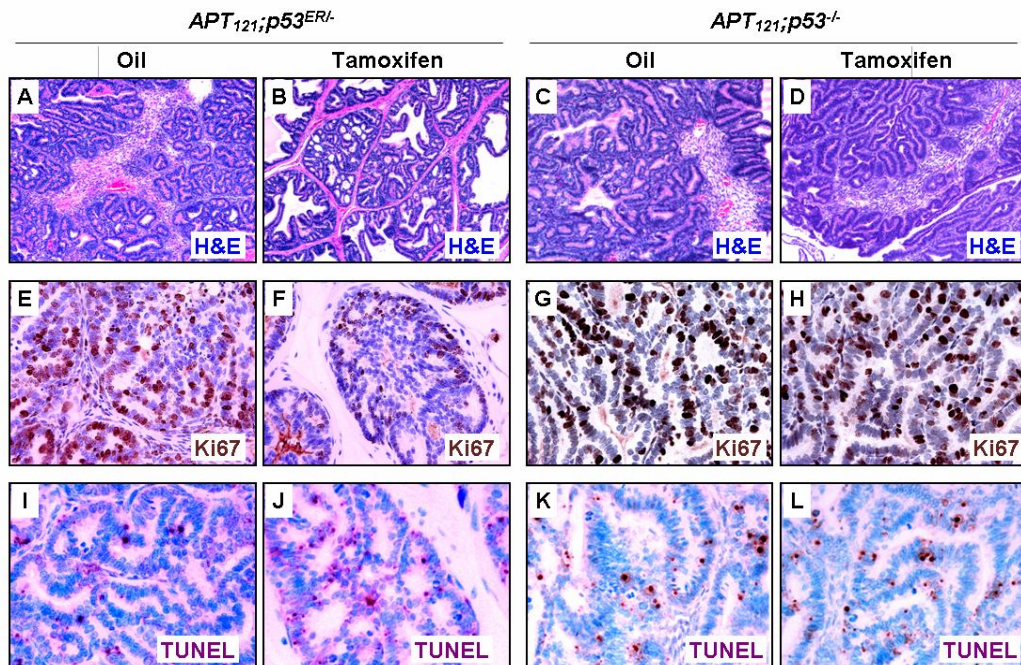
Table 2. Restoration of p53 function in *APT $_{121}$; p53$^{TAM/-}$* mice delays the onset of prostate tumors.

Genotype	IP injection	mPIN	Adenocarcinoma	Stromal Tumor
APT$_{121}$; p53$^{ER/-}$	Oil	0/5	5/5	2/5
APT$_{121}$; p53$^{ER/-}$	Tamoxifen	4/6	2/6	0/6
APT$_{121}$; p53 $^{-/-}$	Oil	0/4	4/4	2/4
APT$_{121}$; p53 $^{-/-}$	Tamoxifen	0/4	4/4	1/4

Discussion

Prostate cancer is a devastating disease that affects adult men and is the second most common cancer among this population. It is predicted that 1 out of 6 men will be diagnosed with prostate cancer during their lifetime (58). Over the last few years, many research groups have developed animal models to analyze the stages and progression of the disease. However, the heterogeneous nature of prostate cancer has proven difficult to recapitulate. One useful model to study the progression of prostate cancer is the APT_{121} transgenic mouse. In this model, the expression of Rb and its family members, p107 and p130, is inhibited upon expression of the N-terminal fragment of the SV40 T antigen, which is regulated in this model by the prostate epithelial-specific probasin promoter. APT_{121} mice have normal expression of p53, making these mice suitable for studying the role of Rb as a cancer initiator to which other mutations can be added in order to understand the multistage nature of the disease.

In this study, we have deleted p53 somatically in prostate epithelial cells in order to better recapitulate the progression of human prostate cancer. In particular, we took advantage of the APT_{121} mouse model to mimic the initial aberrant event in the development of prostate neoplasia and then induced somatic inactivation of p53 by generating $APT_{121};p53^{cf/f};Pb\text{-}Cre$ compound animals. Here, we were able to demonstrate that $APT_{121};p53^{cf/f};Pb\text{-}Cre$ mice, similar to the previously reported $APT_{121};p53^{-/-}$ mice, develop adenocarcinomas much earlier and at a higher incidence than APT_{121} transgenic mice. Furthermore, the $APT_{121};p53^{cf/f};Pb\text{-}Cre$ tumors also recapitulated the appearance of stromal tumors, which have been previously described in the $APT_{121};p53^{-/-}$ mouse model. Stromal tumors, although

51

rare, are a clinical challenge during the development of human prostate malignancies, due to the uncommon pattern of proliferation that results in various histological presentations. These tumors, also known as Stromal Tumors of Uncertain Malignant Potential (STUMP), present a unique pattern of proliferation in these stromal cells, which are behaviorally and histologically distinct from benign hyperplasias and whose behavior cannot be predicted by histological appearance. In this case, we found that the $APT_{121};p53^{cf/f};Pb$-Cre tumors were greatly enlarged, in part due to uncontrolled proliferation and expansion of the mesenchymal compartment (Figure 1E-F). These results indicate that p53 deletion in prostate epithelium with a compound loss of Rb function is sufficient to drive prostate tumorigenesis and stromal-associated malignant transformation. Furthermore, the data presented here suggest that the stromal tumors observed in a previous study (18, 51) in $APT_{121};p53^{+/-}$ and $APT_{121};p53^{-/-}$ prostates could be the result of paracrine signals induced by the epithelial cells to the stroma, rather than a consequence of cell-autonomous loss of p53 in the stroma. However, whether this is actually true remains to be determined.

Another interesting finding from this study is that tumors derived from $APT_{121};p53^{cf/f};Pb$-Cre mice display increased proliferation compared to APT_{121} tumors, but without noticeable changes in apoptotic levels. p53-independent apoptosis in prostate tumors has been demonstrated in the APT_{121} model (18). Here, we found evidence that p53 ablation enhances the over-proliferative phenotype induced by loss of Rb function in prostate epithelial cells, which may cause the early onset of prostate cancer. Furthermore, we evaluated the dependency of the APT_{121} tumors on p53 activity by utilizing the $APT_{121};p53^{ER/-}$

mouse model. In this case, restoration of p53 activity by administration of tamoxifen resulted in decreased proliferation and increased apoptosis in the prostate and significantly reduced tumor progression. In this scenario, p53-dependent apoptosis clearly play a role in the prevention of the malignant phenotype, which is different from the results obtained with *APT$_{121}$;p53$^{cf/f}$;Pb-Cre* mice*. A possible explanation is that in *APT$_{121}$;p53$^{cf/f}$;Pb-Cre* mice, prostate cells are able to adapt to the absence of p53, whereas in tamoxifen-treated *APT$_{121}$;p53$^{ER/-}$* mice, rapid restoration of p53 induces apoptosis. It is likely that epithelial deletion of the *p53* gene is sufficient to drive malignant transformation and the development of surrounding stromal neoplasias. As the cells undergo aberrant proliferation, there may be selection pressure for cells that have acquired further mutations leading to genomic instability, resulting in the loss of other genes involved in apoptosis including p53. In summary, our results emphasize the relevance of p53 in mediating prostate cancer and its collaboration with Rb inactivation. Our data suggest that delivery of p53 in the epithelial prostate gland could be a potential therapeutic strategy for treatment of prostate cancers.

Materials and methods

Mouse breeding strategies

To study the somatic deletion of p53 in APT_{121} mice, APT_{121} females were crossed with $p53^{cf/f}$ males to create and select for $APT_{121};p53^{cf/+}$ mice; $p53^{cf/f}$ females were then crossed with *Pb-Cre* males to generate and select for $Pb-Cre;p53^{cf/+}$ males. The $APT_{121};p53^{cf/+}$ females were crossed with $Pb-Cre;p53^{cf/+}$ males to generate $APT_{121};p53^{cf/f};Pb-Cre$ mice and littermate controls without *Pb-Cre*. Similarly, to study the effect of p53 restoration in APT_{121} mice, the mice were mated with $p53^{ER/-}$ and with $p53^{-/-}$ mice. The offspring generated by the breeding, $APT_{121};p53^{ER/-}$ and $APT_{121};p53^{-/-}$ mice, were intraperitoneally injected with oil or tamoxifen (1mg/mouse) once every 3 days for 30 days to restore p53 activity. Prostate tissues were harvested for analysis of tumor development and for measuring proliferation and apoptosis.

Histopathology

Prostate samples were fixed overnight in 10% phosphate-buffered formalin, transferred to 70% ethanol, and then embedded into paraffin. Samples were sectioned for 10 successive layers at 5-μm intervals and stained with H&E for histopathologic examination.

Immunohistochemistry

Immunohistochemical analysis was performed on formalin-fixed, paraffin embedded tumor sections. Detection of antibodies for Ki67 (550609, BD Pharmigen, San Diego, CA) , T121 (Ab-2, Calbiochem, San Diego, CA), Cytokeratin 8/18 (GP11, Progen, Heidelberg,

Deutschland, Germany), α-smooth muscle actin (A2547, Sigma-Aldrich, St. Louis, MO), androgen receptor (PG-21, Upstate, Temecula, CA) and synaptophysin (611880, BD Pharmigen, San Diego, CA) was done using the Vector ABC Elite kit and a Vector 3,3'-Diaminobenzidine kit for substrate detection (Vector Laboratories, Burlingame, CA). Apoptotic levels were assessed using the terminal deoxynucleotidyl transferase–mediated dUTP-biotin nick end labeling (TUNEL) assay (ApopTaq Peroxidease in situ Kit from Chemicon) following the manufacturer's instructions. Cells from 5 random areas of each prostate tumor sample were counted, and the percentage of positively stained cells compared to the total number of cells was calculated. Differences in proliferation or apoptosis levels among mice of all genotypes were evaluated using a t-test ($P < 0.05$ was considered of statistical significance).

CHAPTER THREE

The *in vivo* Role of the RP-Mdm2-p53 Pathway in Signaling Oncogenic Stress Induced by pRb Inactivation and Ras Overexpression

Abstract

The Mdm2-p53 tumor suppression pathway plays a vital role in regulating cellular homeostasis by integrating a variety of stressors and eliciting effects on cell growth and proliferation. Recent studies have demonstrated an *in vivo* signaling pathway mediated by ribosomal protein (RP)-Mdm2 interaction that responds to ribosome biogenesis stress and evokes a protective p53 reaction. It has been shown that mice harboring a Cys-to-Phe mutation in the zinc finger of Mdm2 that specifically disrupts RP L11-Mdm2 binding are prone to accelerated lymphomagenesis in an oncogenic c-Myc driven mouse model of Burkitt's lymphoma. Because most oncogenes when upregulated simultaneously promote both cellular growth and proliferation, it therefore stands to reason that the RP-Mdm2-p53 pathway might also be essential in response to oncogenes other than c-Myc. Using genetically engineered mice, we now show that disruption of the RP-Mdm2-p53 pathway by an $Mdm2^{C305F}$ mutation does not accelerate prostatic tumorigenesis induced by inactivation of the pRb family proteins (pRb/p107/p130). In contrast, loss of p19Arf greatly accelerates the progression of prostate cancer induced by inhibition of pRb family proteins. Moreover, using ectopically expressed oncogenic H-Ras we demonstrate that p53 response remains intact in the $Mdm2^{C305F}$ mutant MEF cells. Thus, unlike the p19Arf-Mdm2-p53 pathway,

which is considered a general oncogenic response pathway, the RP-Mdm2-p53 pathway appears to specifically suppress the tumorigenesis induced by oncogenic c-Myc.

Acknowledgement

Introduction

p53 is a critical tumor suppressor gene which is mutated in about 50% of all human tumors (23). It is often referred to as the guardian of the genome because under various cellular stress conditions such as DNA damage, oncogenic insult, and hypoxia, p53 is stabilized and activated, inducing cell cycle arrest, apoptosis, DNA damage repair, senescence, and a variety of other protective responses (21). Under normal conditions, p53 levels are kept low, mainly through inhibition by Mdm2 (mouse double minute 2). The C-terminus of Mdm2 has an intrinsic E3 ligase activity, which promotes the ubiquination and degradation of p53. The N-terminus of Mdm2 binds to the transactivation domain of p53 and inhibits the recruitment of co-activators. Mdm2 is also directly transactivated by p53, therefore forming an Mdm2-p53 feedback loop to maintain cellular homeostasis (22).

Recently several ribosomal proteins, including L11 (59), L5 (34) and L23 (33, 60) have been shown to bind Mdm2 at its zinc finger domain. Under normal conditions, these proteins, along with rRNAs, form the large and small subunits of ribosomes in the nucleolus (25). However, under conditions of ribosome stress, free forms of ribosomal proteins are released into the nucleoplasm and bind to Mdm2, leading to p53 stabilization and activation (61). A cancer-associated cysteine-to-phenylalanine point mutation in the zinc finger domain of Mdm2 causes disruption of L11 and L5 binding to Mdm2 (62), and based on this *in vitro* data, we previously generated a knock-in mouse with the Mdm2 C305F mutation. Mdm2^{C305F} mutant mice maintain a normal p53 response to DNA damage, but are deficient in p53 induction in response to induced ribosomal stress (40).

Intriguingly, the Mdm2 C305F mutation was recently shown to significantly accelerate B cell lymphomagenesis in an Eμ-Myc induced mouse model of B cell lymphoma (40). The ability of Myc to promote cell growth and proliferation is closely linked to its role in regulating ribosomal biogenesis. Myc facilitates the recruitment of Pol I to rDNA promoters (63-64), promotes the transcription of ribosomal proteins by activating Pol II (65-68), and activates Pol III-mediated

58

transcription of 5S rRNA and tRNA (69). In the case of Eµ-myc-induced lymphoma, ribosomal proteins L11 and L5 are unable to bind and suppress Mdm2^{C305F} in Eµ-*Myc;Mdm2*$^{C305F/C305F}$ mice, and as a result activation of p53 is attenuated and B cell lymphomagenesis is accelerated (40). These findings established the RP-Mdm2-p53 pathway as a genuine barrier to Myc-induced tumorigenesis.

Another well-studied pathway suppressing Myc-induced B cell lymphoma is ARF-Mdm2-p53 signaling. Loss of p19Arf results in a similar acceleration of Eµ-Myc induced lymphomagenesis to that caused by Mdm2 C305F mutation (40, 44). ARF can physically interact with Mdm2, and therefore, releasing p53 from Mdm2-mediated degradation and transactivation silencing (70-73). Besides Myc, ARF can also induce p53 in response to E2F1 and Ras. E2F1 directly activates human p14Arf at transcriptional level(74).Overexpression of Ras transforms p19 null mouse embryo fibroblasts (MEFs) via bypassing p53-mediated checkpoint control (75). Ras induces a cell cycle arrest in wild type murine keratinocytes, which mediated by an increased expression of p19Arf (76). While ARF-Mdm2-p53 signaling acts downstream of a variety of oncogenes, that ARF-independent induction of p53 can also occur upon oncogenic stress. For instance, when expressing T121, a transgene inhibiting pRb and therefore activating E2F1, in choroid plexus (CP) epithelial cells, p19Arf is dispensable for p53-mediated tumor suppression and apoptosis (77). Ras induction of p53-dependent cell cycle arrest in murine keratinocytes also does not rely on ARF (78). The alternative pathway leading to p53 activation is unclear. Given that oncogenes promote cell proliferation and/or growth associated with elevated protein synthesis, ribosomal biogenesis might be generally disrupted in response to oncogenic stress. Therefore, RP-Mdm2-p53 signaling may play a general role in responding to oncogenic stress and suppressing tumorigenesis like it does in Myc-induced B cell lymphoma.

E2F1 has been reported to bind rRNA promoter and enhance its activity (79). Similarly, in the yeast *Saccharomyces cerevisiae*, Ras/TOR induces Sfp1 which is required for

Ifh1(transcriptional co-activator) binding to RP gene promoters, a network linking cell growth to ribosomal biogenesis (80). In the mammalian cell, maRas-PI3K-Akt-mTOR is well-known to promote protein translation and cell growth (81). All these cellular process may induce ribosomal stress, which leads to activation of RP-Mdm2-p53 signaling. Hence, the current study focuses on examining whether the RP-Mdm2-p53 pathway may act as a general response to oncogenic stress by utilizing models of pRb inactivation and Ras activation.

Specifically, to investigate whether disruption of RP-Mdm2-p53 signaling accelerates tumorigenesis induced by inactivation of pRb, we crossed $Mdm2^{C305}$ mice with a well-characterized mouse prostate cancer model called APT_{121}, in which a truncated SV40 large T antigen under the probasin promoter leads to pRb inactivation in prostate epithelium (18, 82), to see if tumor progression is accelerated by $Mdm2^{C305}$.To investigate whether disruption of RP-Mdm2-p53 signaling accelerates tumorigenesis induced by Ras activation, we used normal mouse keratinocytes and mouse embryonic fibroblasts (MEFs) systems to measure the ribosomal proteins and compare p53 response signaling.

Results

Mdm2 C305F mutation causes reduced prostate size and slows the progression of APT_{121}-induced prostate cancer

Inactivation of p53 alone in the murine prostate leads to the development of prostatic intraepithelial neoplasia (PIN) with no progression to invasive carcinoma, suggesting that loss of p53 may be a complementary rather than initiating event in promoting prostate tumorigenesis (83). Previous findings have also shown that attenuation of p53 signaling through loss of one allele of p53 does not accelerate the onset of epithelial tumors in an APT_{121}-induced mouse model of prostate cancer, but induces a stromal tumor phenotype, which is characterized by extensive stromal cell presence and intraductal growth patterns (51). The Mdm2 C305F mutation, which disrupts the binding of ribosomal proteins L11 and L5 to Mdm2 (40), causes an attenuation of p53 signaling, suggesting that the Mdm2 C305F mutation may alter the progression, rather than initiation, of prostate tumorigenesis in a similar way as p53 heterozygosity.

To examine the importance of the RP-Mdm2-p53 pathway in APT_{121}-induced prostate cancer, we generated $APT_{121};Mdm2^{+/+}$ and $APT_{121};Mdm2^{C305F/C305F}$ mice and non-tumorigenic control $Mdm2^{+/+}$ and $Mdm2^{C305F/C305F}$ mice. The progression of tumorigenesis was then compared among these mice to see if disruption of RP-Mdm2-p53 signaling altered the development of cancer.

$APT_{121};Mdm2^{+/+}$ and $APT_{121};Mdm2^{C305F/C305F}$ mice did not exhibit noticeable differences in general appearance or body weight. We compared the size of prostate glands isolated

from mice at 6 months of age. Surprisingly, the prostates from $Mdm2^{C305F/C305F}$ mice were generally smaller than those from $Mdm2^{+/+}$ mice, and consistent with this finding, the prostates from $APT_{121};Mdm2^{C305F/C305F}$ mice were smaller than those from $APT_{121};Mdm2^{+/+}$ mice (Figure 14A). The average weight of 11 $Mdm2^{C305F/C305F}$ prostates was 0.088 grams while that of 12 $Mdm2^{+/+}$ prostates was 0.117 grams. The average weight of 13 $APT_{121};Mdm2^{C305F/C305F}$ prostates was 0.172 grams and that of 9 $APT_{121};Mdm2^{+/+}$ prostates was 0.221 grams (Figure 14B). The differences in weight were statistically significant, with *p < 0.05 and **p < 0.01 respectively.

We next examined prostate histology by hematoxylin and eosin (H&E) staining on paraffin-embedded prostate samples isolated from 6 month-old mice. None of the $Mdm2^{C305F/C305F}$ or $Mdm2^{+/+}$ mice exhibited abnormality in their prostates (Figure 14C). Prostate adenocarcinoma, defined as penetration of malignant prostate epithelial cells through the basement membrane of the prostate gland into the surrounding stroma, was often observed in $APT_{121};Mdm2^{+/+}$ mice, while the majority of the $APT_{121};Mdm2^{C305F/C305F}$ mice only developed mPIN (mouse prostatic intraepithelial neoplasia), with few examples of well-differentiated adenocarcinoma (Figure 14C). As shown in Table 3, 71.4% of $APT_{121};Mdm2^{+/+}$ mice developed adenocarcinomas compared with only 37.5% of $APT_{121};Mdm2^{C305F/C305F}$ mice. Thus the progression from mPIN to adenocarcinoma is decreased by $Mdm2^{C305F}$ mutation.

Figure 14. Mdm2 C305F mutation causes reduced prostate size and slows the progression of APT_{121}-induced prostate cancer.

A. Photographs showing representative prostates from 6 month-old mice of the indicated genotypes.

B. Average prostate mass ± SD from 6 month-old mice of the indicated genotypes. $Mdm2^{+/+}$ (n=12), $Mdm2^{C305F/C305F}$ (n=11), $APT_{121};Mdm2^{+/+}$ (n=9), and $APT_{121};Mdm2^{C305F/C305F}$ (n=13) . * p < 0.05 and ** p < 0.01   as assessed by Student's t test.

C. Representative H&E staining of prostate sections from 6 month-old mice of the indicated genotypes demonstrating histology associated with the indicated stages of tumor progression. Scale bar was shown in the first picture and all pictures were taken at the same magnification.

A

Mdm2$^{+/+}$

Mdm2$^{C305F/C305F}$

APT$_{121;}$Mdm2$^{+/+}$

APT$_{121;}$Mdm2$^{C305F/C305F}$

B

Average Prostate Mass (grams)

*p<0.05

**p<0.01

Mdm2$^{+/+}$

Mdm2$^{C305F/C305F}$

APT$_{121}$ Mdm2$^{+/+}$

APT$_{121}$ Mdm2$^{C305F/C305F}$

C

Normal

mPIN

Adenocarcinoma

50μM

Mdm2$^{+/+}$

APT$_{121;}$Mdm2$^{+/+}$

Normal

mPIN

Adenocarcinoma

Mdm2$^{C305F/C305F}$

APT$_{121;}$Mdm2$^{C305F/C305F}$
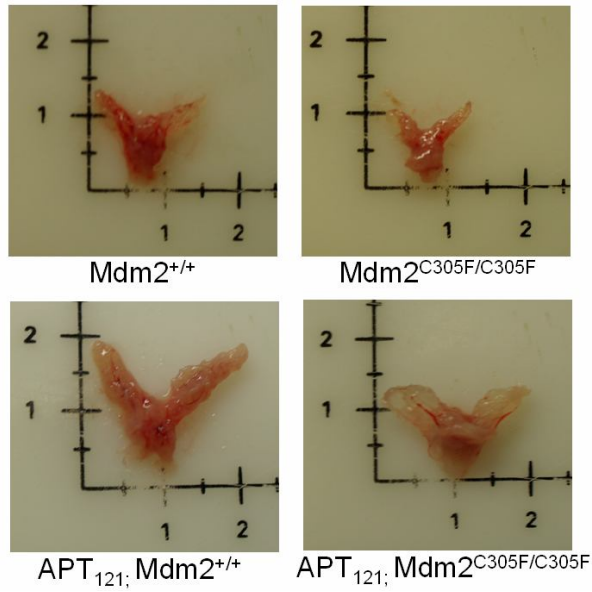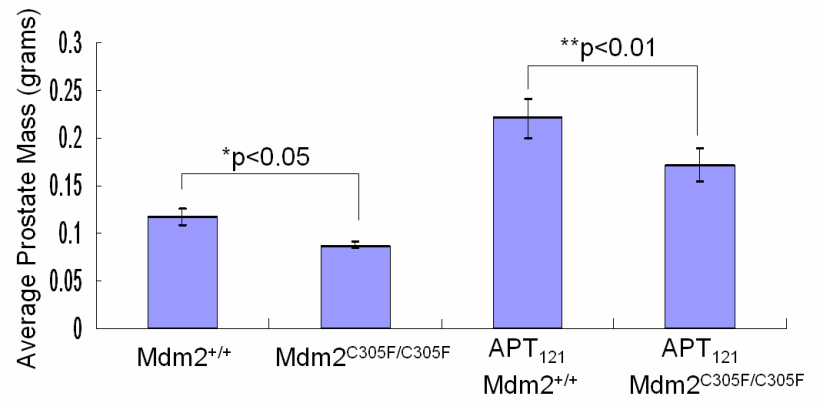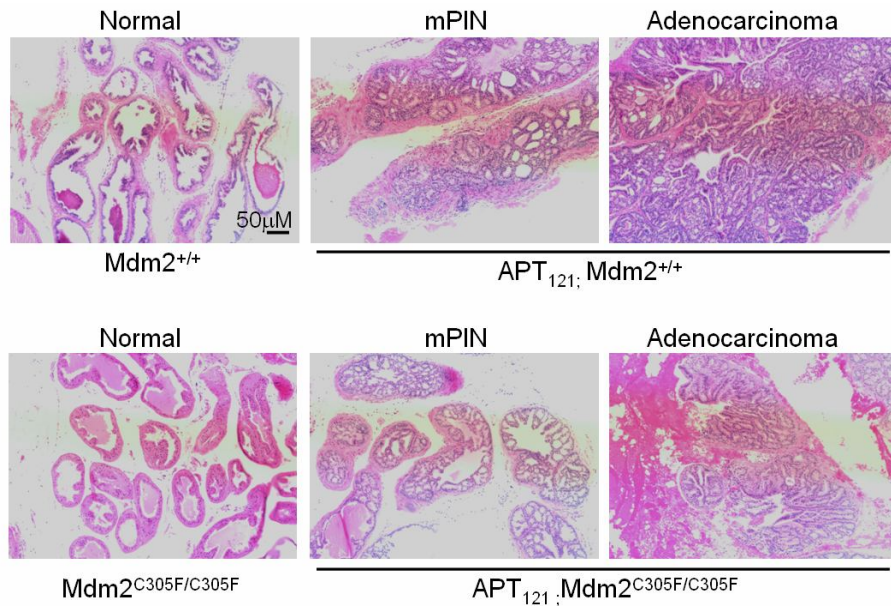
Table 3. Summary of prostate tumor stages in 6 month-old *Mdm2$^{+/+}$, Mdm2$^{C305F/C305F}$,*

APT$_{121}$;Mdm2$^{+/+}$, **and** *APT$_{121}$; Mdm2$^{C305F/C305F}$* **mice.**

	Mdm2$^{+/+}$	Mdm2$^{C305F/C305F}$	APT$_{121}$;Mdm2$^{+/+}$	APT$_{121}$; Mdm2$^{C305F/C305F}$
Total	8	7	7	8
Normal	8	7	0	0
Dysplasia	0	0	0	0
mPIN	0	0	2	5
Adenocarcinoma	0	0	5 (71.4%)	3 (37.5%)

Mdm2 C305F mutation decreases proliferation but does not affect apoptosis of APT_{121}-induced prostate cancer

To address the differences in tumor progression described above, the proliferation and apoptosis of isolated prostate tissues were examined by immunohistochemical analysis. Cell proliferation was assessed by ki67 staining. Prostates from $Mdm2^{C305F/C305F}$ or $Mdm2^{+/+}$ mice had few proliferating cells, while prostates from $APT_{121};Mdm2^{+/+}$ and $APT_{121};Mdm2^{C305F/C305F}$ mice were highly proliferative (Figure 15A). As quantified in Figure 15B, there was no statistically significant difference in the percentage of ki67 positive cells between $Mdm2^{+/+}$ and $Mdm2^{C305F/C305F}$ prostates (3.64% and 3.39%, respectively). However, there was a statistically significant difference in the percentage of ki67 positive cells between $APT_{121};Mdm2^{+/+}$ and $APT_{121};Mdm2^{C305F/C305F}$ prostates (64.6% and 48.8%, respectively).

To examine apoptosis in the prostates of the various transgenic mice, TUNEL (terminal deoxynucleotidyl transferase–mediated dUTP-biotin nick end labeling) immunohistochemical analysis was carried out. Representative pictures of TUNEL-stained sections are shown in Figure 15C. Prostates isolated from $APT_{121};Mdm2^{+/+}$ and $APT_{121};Mdm2^{C305F/C305F}$ mice had a much higher percentage of TUNEL-positive apoptotic cells than those of $Mdm2^{+/+}$ or $Mdm2^{C305F/C305F}$ mice (Figure 15D). However, there was no significant difference in apoptosis between $APT_{121};Mdm2^{+/+}$ and $APT_{121};Mdm2^{C305F/C305F}$ prostates (5.59% and 6.51% respectively) or between $Mdm2^{+/+}$ and $Mdm2^{C305F/C305F}$ prostates (0.29% and 0.89% respectively). Taken together, these data suggest that the $Mdm2^{C305F}$ mutation may slow down the progression of prostate tumorigenesis by decreasing proliferation, rather than affecting the apoptosis of prostatic cells.

Previous studies have shown that Myc can up-regulate ribosomal biogenesis (63-64) and that ribosomal protein expression is elevated during Myc-induced lymphomagenesis (40). To investigate whether APT_{121} induces increased expression of ribosomal proteins, total protein was isolated from prostate glands harvested from four mice of each genotype, and

expression of ribosomal protein L11 was examined by western blot. Unlike the situation in Myc-induced lymphomagenesis in which L11 was significantly increased in the presence of Myc (40), L11 was not induced by APT_{121} (data not shown), suggesting that APT_{121}-induced prostate cancer does not cause ribosomal stress.

Figure 15. Mdm2 C305F mutation decreases proliferation but does not affect apoptosis of *APT$_{121}$*-induced prostate cancer.

A. Representative Ki67 staining of prostate sections from 6 month-old mice of the indicated genotypes. Brown staining indicates proliferating cells. Scale bar was shown in the first picture and all pictures were taken at the same magnification.

B. Average % Ki67-positive cells ± SD from 6 month-old mice of the indicated genotypes. At least five independent fields consisting of a total of at least 1,000 cells from each prostate sample were counted. **$p < 0.01$ as assessed by Student's t test.

C. Representative TUNEL staining of prostate sections from 6 month-old mice of the indicated genotypes. Brown staining indicates apoptotic cells. Scale bar was shown in the first picture and all pictures were taken at the same magnification.

D. Average % TUNEL-positive cells ± SD from 6 month-old mice of the indicated genotypes. At least five independent fields consisting of a total of at least 1,000 cells from each prostate sample were counted. (A – D) *Mdm2$^{+/+}$* (n=8)*, Mdm2$^{C305F/C305F}$* (n=7), *APT$_{121}$;Mdm2$^{+/+}$* (n=7), and *APT$_{121}$;Mdm2$^{C305F/C305F}$* (n=9) mice were used.

A
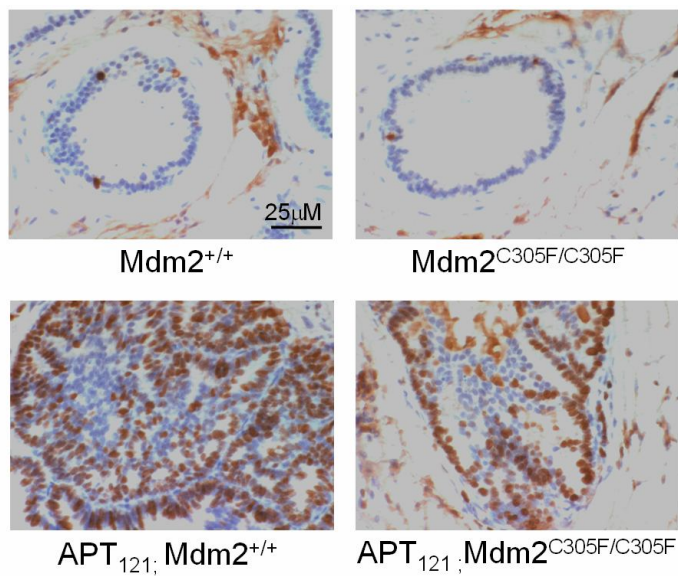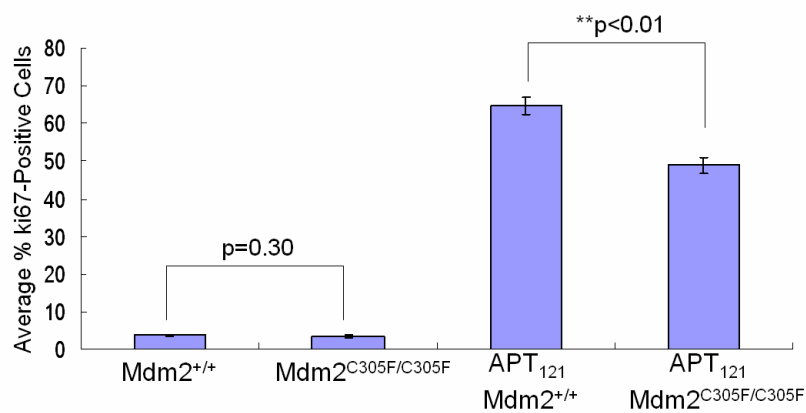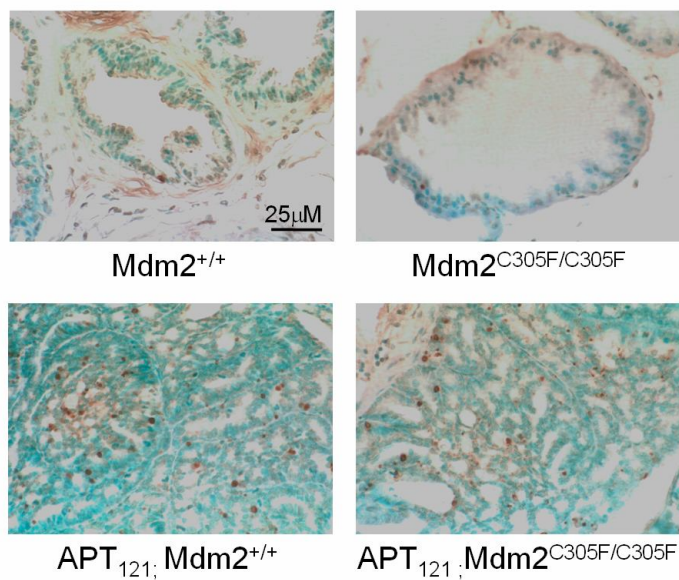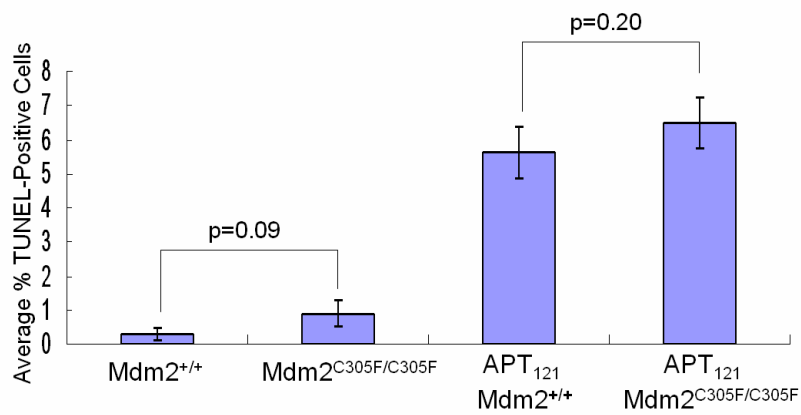
Mdm2$^{+/+}$

Mdm2$^{C305F/C305F}$

APT$_{121}$;Mdm2$^{+/+}$

APT$_{121}$;Mdm2$^{C305F/C305F}$

25μM

B

Average % ki67-Positive Cells

**p<0.01

p=0.30

Mdm2$^{+/+}$ Mdm2$^{C305F/C305F}$ APT$_{121}$ Mdm2$^{+/+}$ APT$_{121}$ Mdm2$^{C305F/C305F}$

C

Mdm2$^{+/+}$

Mdm2$^{C305F/C305F}$

APT$_{121}$;Mdm2$^{+/+}$

APT$_{121}$;Mdm2$^{C305F/C305F}$

25μM

D

Average % TUNEL-Positive Cells

p=0.20

p=0.09

Mdm2$^{+/+}$ Mdm2$^{C305F/C305F}$ APT$_{121}$ Mdm2$^{+/+}$ APT$_{121}$ Mdm2$^{C305F/C305F}$

Loss of p19Arf accelerates adenocarcinoma and stromal tumor development in APT_{121}-induced prostate cancer

While our data suggest that RP-Mdm2 signaling does not inhibit APT_{121}-induced prostate cancer, previous findings have shown that both RP-Mdm2 and p19Arf-Mdm2 signal to p53 and function equivalently as barriers to suppress Myc-induced B cell lymphoma (40, 44). ARF can be induced by a variety of oncogenes including Ras, Myc and E2F1, inhibiting Mdm2 and thereby activating p53 (74, 84-85). p53 is believed to play an important role in suppressing prostate cancers of higher tumor stage or androgen-independent tumors (86-87). However, it is unknown whether p19Arf-Mdm2-p53 signaling is needed for the suppression of APT_{121}-induced prostate cancer.

To examine the role of the p19Arf-Mdm2-p53 pathway in APT_{121}-induced prostate cancer, we crossed APT_{121} with *p19Arf*-null mice. By 5 months of age, all $APT_{121};p19Arf^{-/-}$ mice developed adenocarcinomas, while the majority of the $APT_{121};p19Arf^{+/+}$ mice only developed mPIN (Table 4). Furthermore, tumors from $APT_{121};p19Arf^{-/-}$ prostates were comprised of a large portion of stromal cells, which expanded not only outside of the epithelial glands, but inside the glands as well (Figure 16A). This phenotype was similar to what was defined as 'stromal tumor' in a previous study (51). The stromal tumor phenotype occurred at a high frequency (5 of 6 mice) in $APT_{121};p19Arf^{-/-}$ mice while it was not detected in $APT_{121};p19Arf^{+/+}$ mice (Table 4).

We further measured the proliferation and apoptosis rates of $APT_{121};p19Arf^{+/+}$ and $APT_{121};p19Arf^{-/-}$ prostates by immunohistochemical analysis as mentioned above. $APT_{121};p19Arf^{-/-}$ prostates exhibited a higher rate of proliferation and no significant difference in apoptosis compared with $APT_{121};p19Arf^{+/+}$ prostates (Figure 16B-C and 16D-E). Therefore, p19Arf-Mdm2-p53 signaling apparently inhibits the progression of APT_{121}-induced prostate cancer by affecting cell proliferation. Taken together, these data suggest that the p19Arf-Mdm2-p53 pathway, rather than the RP-Mdm2-p53 pathway, is the main barrier to

suppress APT_{121}-induced prostate cancer.

**Figure 16. Effects of p19Arf loss on tumor progression in *APT$_{121}$*-induced prostate cancer.**

A. Representative H&E staining of prostate sections from 5 month-old mice of the indicated genotypes. Stromal tumor was detected only in *APT$_{121}$*;p19Arf$^{-/-}$ mice as indicated by asterisk. Scale bar was shown in the first picture and all pictures were taken at the same magnification.

B. Representative Ki67 staining from 5 month-old mice of the indicated genotypes. Scale bar was shown in the first picture and all pictures were taken at the same magnification.

C. Average % Ki67-positive cells ± SD from 5 month-old mice of the indicated genotypes. n=6 for each genotype. At least five independent fields consisting of a total of at least 1,000 cells from each prostate sample were counted. Brown staining indicates proliferating cells. *p = 0.01 as assessed by Student's t test.

D. Representative TUNEL staining from 5 month-old mice of the indicated genotypes. Scale bar was shown in the first picture and all pictures were taken at the same magnification.

E. Average % TUNEL-positive cells ± SD from 5 month-old mice of the indicated genotypes. n=6 for each genotype. At least five independent fields consisting of a total of at least 1,000 cells from each prostate sample were counted. Brown staining indicates apoptotic cells.

A

APT$_{121}$;p19Arf$^{+/+}$ APT$_{121}$;p19Arf$^{-/-}$

50μM

B

ki67

APT$_{121;}$ p19Arf$^{+/+}$ APT$_{121;}$ p19Arf$^{-/-}$

25μM

C

*p=0.01

Average % ki67-Positive Cells

APT$_{121;}$ p19Arf$^{+/+}$ APT$_{121;}$ p19Arf$^{-/-}$

D

TUNEL

APT$_{121;}$ p19Arf$^{+/+}$ APT$_{121;}$ p19Arf$^{-/-}$

25μM

E

p=0.38

Average % TUNEL-Positive Cells

APT$_{121;}$ p19Arf$^{+/+}$ APT$_{121;}$ p19Arf$^{-/-}$
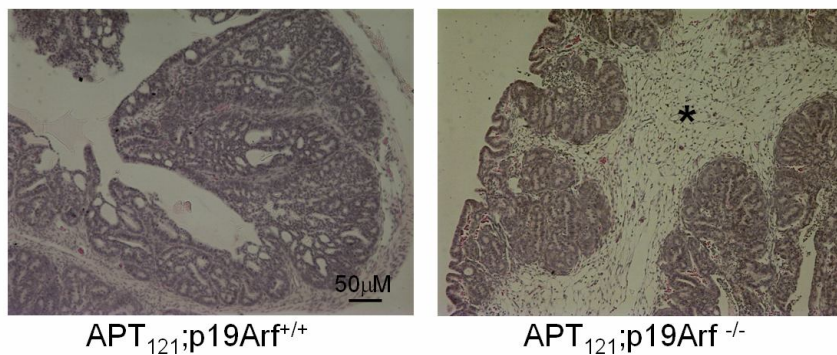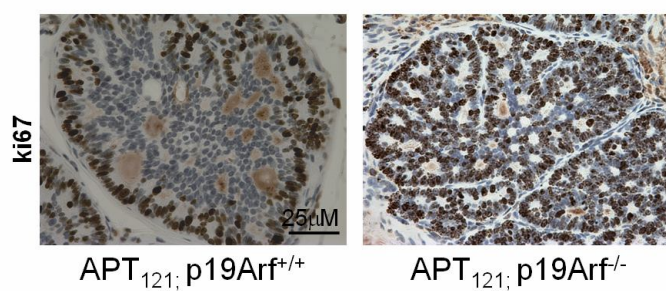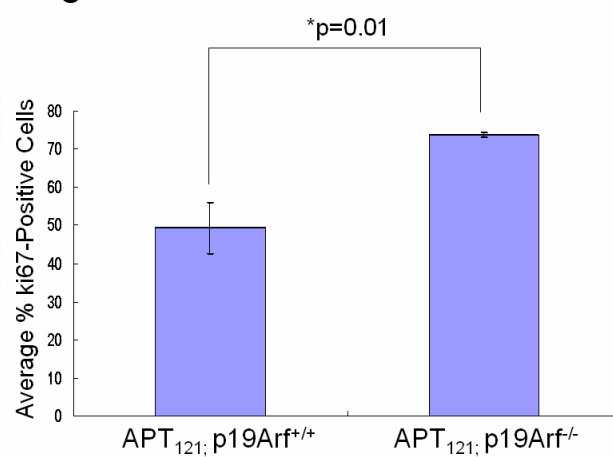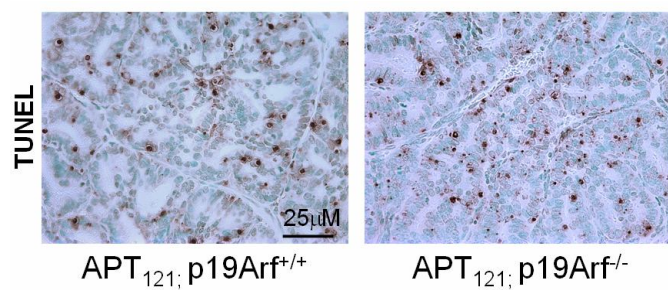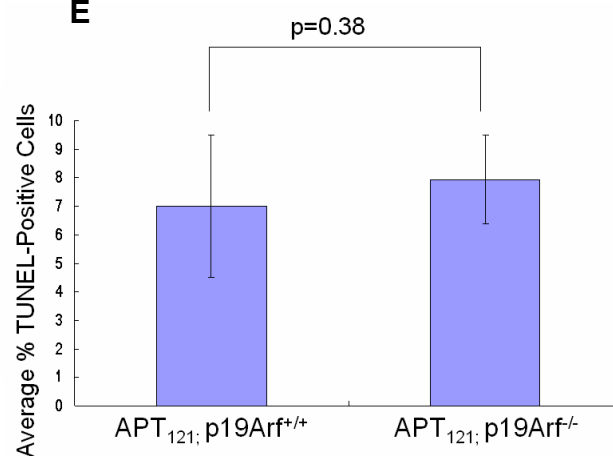
Table 4. Summary of prostate tumor stages in 5 month-old APT_{121};p19Arf$^{+/+}$ and APT_{121};p19Arf$^{-/-}$ mice.

		APT_{121};p19Arf$^{+/+}$	APT_{121};p19Arf$^{-/-}$
Total		**6**	**6**
Epithelial neoplasia	**mPIN**	4	0
	Adenocarcinoma	2 (33.3%)	6 (100%)
Stromal tumor		0	5 (83.3%)

Activated Ras does not up-regulate the expression of ribosomal protein in mouse keratinocytes

To further investigate if the RP-Mdm2-p53 signaling pathway is required for oncogenic Ras induction of p53, we examined its function in response to activation of H-Ras. Constitutively active mutant forms of the Ras family of small GTPases are found in approximately one-third of all human cancers. Active GTP-bound Ras stimulates numerous effector proteins to induce diverse downstream signaling events affecting cell growth, proliferation, differentiation, and apoptosis (88). Given that the Ras-PI3K-Akt-mTOR pathway promotes protein translation and cell growth in mammalian cells (89), we tested whether activated Ras could induce ribosomal stress and trigger the RP-Mdm2-p53 pathway.

To investigate this possibility, we first examined whether Ras could up-regulate the expression of ribosomal proteins in four different mouse keratinocyte cell lines: BalMk2 normal mouse keratinocytes with wild-type Ras, 308 benign mouse skin papilloma cells (90), CH72-T3 malignant mouse skin squamous cell carcinoma cells (91), and CC4A malignant mouse skin carcinoma cells all carrying an H-Ras mutation at codon 61 (92). We measured the protein level of ribosomal protein L11 by western blot. Compared with BalMK2 normal mouse keratinocytes that have wild-type Ras, Ras activation in 308, CH72-T3 or CC4A cell lines did not induce increased expression of ribosomal protein L11 (Figure 17A).

Expression of activated Ras in Mdm2^{C305F} mutant MEFs induces a normal p53 response but does not up-regulate the expression of ribosomal proteins

While the data from mouse keratinocytes suggested that activated Ras may not induce ribosomal stress, the cell lines could not fully address the function of RP-Mdm2-p53 signaling in response to Ras activation. In order to investigate whether the Mdm2^{C305F} mutant protein, and thus decreased interaction between ribosomal proteins and Mdm2, could affect the p53 response to Ras activation, early passage *Mdm2$^{+/+}$* and *Mdm2$^{C305F/C305F}$* MEFs were stably

infected with retroviruses encoding either H-Ras^{G12V} (a constitutively active form of H-Ras) or an empty vector control. Ras is known to induce cellular senescence via an intact p19Arf-Mdm2-p53 pathway in murine cells (75, 84). Following infection with Ras virus, we observed comparable cell cycle arrest in *Mdm2$^{+/+}$* and *Mdm2$^{C305F/C305F}$* MEFs as evidenced by a similar decrease in cell number (Figure 17B). Ras expression was confirmed by western blot analysis and was comparable in *Mdm2$^{+/+}$* and *Mdm2$^{C305F/C305F}$* MEFs (Figure 17C).

To determine the effect of Ras expression on ribosomal protein levels, cell lysates were immunoblotted for expression of L5 and L11. Expression of activated Ras did not upregulate L11 or L5 in *Mdm2$^{C305F/C305F}$* or *Mdm2$^{+/+}$* MEFs (Figure 17C, lane 1 versus lane 2, lane 3 versus lane 4). To examine p53 response to Ras expression, cell lysates were also immunoblotted for p53. Ras induced p53 stabilization in both *Mdm2$^{C305F/C305F}$* and *Mdm2$^{+/+}$* MEFs (Figure 17C, lane1 versus lane2, lane 3 versus lane4). p53 was induced to a similar extent in *Mdm2$^{C305F/C305F}$* and *Mdm2$^{+/+}$* MEFs (Figure 17C, lane2 versus lane4), indicating that *Mdm2$^{C305F/C305F}$* MEFs have a normal p53 response to Ras activation. These data suggest that Ras activation does not induce ribosomal stress in the cells tested, and that RP-Mdm2-p53 signaling may not be critical in response to Ras-induced oncogenic stress.

Figure 17. Activated Ras induces a normal p53 response but does not up-regulate ribosomal protein L11.

A. Detection of L11 and β-actin by immunoblot analysis of total cellular lysate prepared from the indicated mouse karatinocyte cell lines. β-actin serves as a loading control.

B. Representative phase-contrast images of *Mdm2$^{+/+}$* and *Mdm2$^{C305F/C305F}$* MEFs stably infected with empty vector or H-Ras^{G12V} retroviruses.

C. Detection of L11, L5, p53, H-Ras, and β-actin by immunoblot analysis of total cellular lysate prepared from the MEFs described in B. β-Actin serves as a loading control.
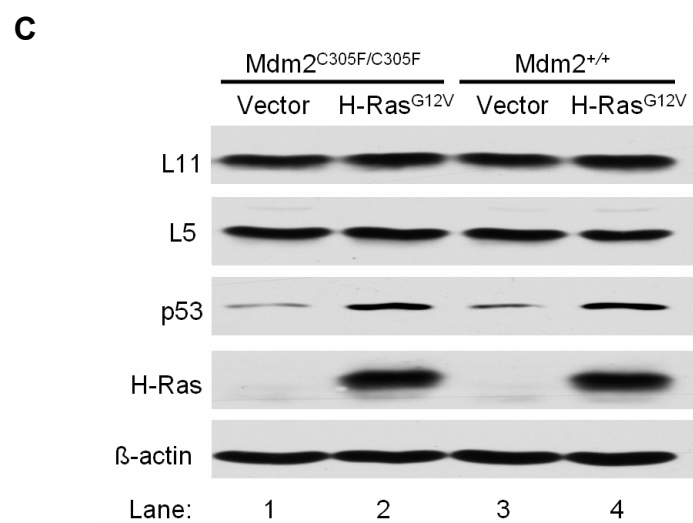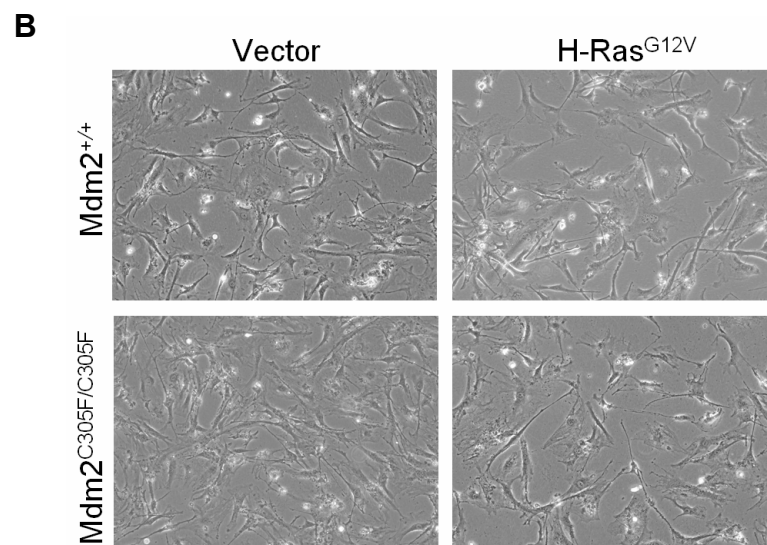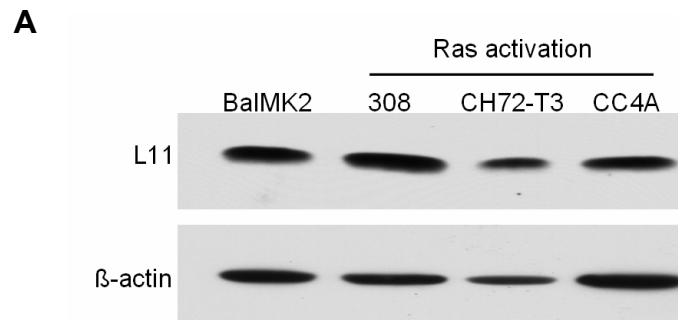
Discussion

Recently several ribosomal proteins, including L11 (59), L5 (34) and L23 (33, 60) have been shown to bind Mdm2 at its zinc finger domain. Under conditions of ribosomal stress, free forms of ribosomal proteins are released into the nucleoplasm and bind to Mdm2, leading to p53 stabilization and activation (61). Interestingly, a cancer-associated cysteine-to-phenylalanine point mutation in the zinc finger domain of Mdm2 disrupts binding of L11 and L5 to Mdm2 (62), and Mdm2^{C305F} mutant knock-in mice are deficient in p53 induction in response to induced ribosomal stress (40).

Additionally, the Mdm2 C305F mutation was recently shown to significantly accelerate B cell lymphomagenesis in an Eμ-Myc induced mouse model of B cell lymphoma (40, 42). The ability of Myc to promote cell growth and proliferation is closely linked to its role in regulating ribosomal biogenesis, and in the case of Mdm2^{C305F} and Myc-induced lymphoma, ribosomal protein expression is elevated, however ribosomal proteins L11 and L5 are unable to bind and suppress Mdm2^{C305F}, resulting in attenuation of p53 activation (40). These findings established the RP-Mdm2-p53 pathway as a genuine barrier to Myc-induced tumorigenesis.

The current study examined whether the RP-Mdm2-p53 pathway acts as a general response to oncogenic stress by utilizing models of pRb inactivation and Ras activation. We now show that Mdm2 C305F mutation results in decreased prostate size and, unlike the situation in Myc-induced B cell lymphomagenesis (40), slows the progression of prostate tumorigenesis induced by inactivation of pRb family proteins in the well-characterized APT_{121} mouse model of prostate cancer (18). Immunohistochemical analysis showed a significant decrease in the percentage of ki67-positive cells in prostates isolated from $APT_{121};Mdm2^{C305F/C305F}$ versus $APT_{121};Mdm2^{+/+}$ mice, but no significant difference in TUNEL staining. These data suggest that the reduction in prostate size and slowed progression of prostate tumorigenesis induced by Mdm2 C305F mutation may be due to a defect in proliferation rather than an increase in cell death. Moreover, unlike the situation in

Myc-induced lymphomagenesis in which ribosomal protein L11 expression was significantly increased (40), L11 expression was not induced by APT_{121} (data not shown), suggesting that APT_{121}-induced prostate cancer does not cause ribosomal stress. Interestingly, $Mdm2^{C305F/C305F}$ mice exhibit smaller prostates than wild-type mice. Need to point out, except for the differences in size, the prostates from $Mdm2^{C305F/C305F}$ mice are completely normal in function and do not have any defects in prostate development. p53 has recently been reported to promote cell survival through induction of *TIGAR* (*T*P53-*i*nduced *g*lycolysis and *a*poptosis *r*egulator) (93). It is possible that disruption of RP-Mdm2-p53 signaling leads to slightly lower level of p53 in the $Mdm2^{C305F/C305F}$ prostates. Under normal condition, the slightly difference in p53 level may not be critical for cell proliferation and growth. However, under oncogenic stress such as pRb inhitition, lower p53 level may hinder cell proliferation in the $Mdm2^{C305F/C305F}$ prostates.

With regard to Ras activation, we show that constitutively active mutant Ras does not up-regulate the expression of ribosomal proteins either in mouse keratinocyte cell lines or when overexpressed in $Mdm2^{+/+}$ or $Mdm2^{C305F/C305F}$ MEFs. These data suggest that Ras activation does not induce ribosomal stress in the cells tested, and that RP-Mdm2-p53 signaling may not be critical in response to Ras-induced oncogenic stress.

While previous findings have shown that both RP-Mdm2 and p19Arf-Mdm2 signal to p53 and similarly suppress Myc-induced B cell lymphoma (40, 44), our data presented here suggest that disruption of RP-Mdm2 signaling does not accelerates APT_{121}-induced prostate cancer. However, loss of p19Arf accelerates adenocarcinoma and stromal tumor development in APT_{121}-induced prostate cancer, and isolated $APT_{121};p19Arf^{-/-}$ prostates exhibited a higher rate of proliferation and no significant difference in apoptosis compared with $APT_{121};p19Arf^{+/+}$ prostates. Thus, p19Arf-Mdm2-p53 signaling apparently inhibits APT_{121}-induced prostate cancer progression by affecting cell proliferation. Furthermore, the phenotype observed in $APT_{121};p19Arf^{-/-}$ mice is consistent with that reported in a prior study

80

on *APT$_{121}$;p53$^{-/-}$* mice (51), confirming the importance of p19Arf-Mdm2-p53 signaling in tumor suppression of *APT$_{121}$*-induced prostate cancer.

In conclusion, the present study suggests that the p19Arf-Mdm2-p53 pathway suppresses *APT$_{121}$*-induced prostate tumorigenesis. p19Arf-Mdm2-p53 may be a general pathway to suppress a wide range of oncogenic assaults.. However, p19Arf is not required for p53 response to ribosomal stress while RP-Mdm2-p53 signaling is required (40). The lack of ribosomal stress observed upon pRb inactivation and Ras activation also suggests that the PR-Mdm2-p53 pathway may not be a general barrier to oncogenic stress, but rather a specific response to ribosomal stress induced by oncogenes such as Myc. It is likely that p19Arf and RP are induced by different cellular stress and therefore, binds to Mdm2 and activates p53，which emphasizes the importance of Mdm2 in mediating p53 response upon a variety of cellular stresses, such as oncogenic stress and ribosomal stress.

Materials and methods

Ethics Statement

This study is approved by the Institutional Animal Care and Use Committee at the University of North Carolina at Chapel Hill. IACUC approval ID. 10-045.0. Mice were humanely euthanized by CO_2 asphyxiation followed by a second method to ensure euthanasia. Mouse tumors and organs were fixed in formalin for histopathology and snap frozen for protein extraction.

Mouse Breeding Strategies

Derivation of APT_{121} (C57BL6/J;DBA2) transgenic mice was previously described (18). To study the effect of the RP-Mdm2-p53 pathway on prostate tumorigenesis, APT_{121} mice were mated to $Mdm2^{C305F/C305F}$ (C57BL6/J) mice that were generated and genotyped as previously described (40). We used standard breeding strategies to produce $APT_{121};Mdm2^{+/+}$, $APT_{121};Mdm2^{C305F/C305F}$ and nontransgenic male littermates $Mdm2^{+/+}$ and $Mdm2^{C305F/C305F}$ served as controls. To study the effect of the p19Arf-Mdm2-p53 pathway on prostate tumorigenesis, APT_{121} mice were mated to $p19Arf^{-/-}$ (C57BL6/J; Sv129) mice that were generated and genotyped as previously described (75). Mice harboring a homozygous deletion of $p19^{ARF}$ exon 1 were originally provided by C. J. Sherr and M. F. Roussel (St. Jude Children's Hospital) and maintained in Terry Van Dyke's lab (UNC-Chapel Hill). We used standard breeding strategies to produce $APT_{121};p19^{ARF+/+}$ and $APT_{121};p19^{ARF-/-}$ mice. Mice were bred and maintained under a protocol (10-045.0) approved by the Institutional Animal Care and Use Committee at the University of North Carolina Animal Care Facility. Mice were humanely euthanized by CO_2 asphyxiation followed by a second method to ensure euthanasia. Mouse tumors and organs were fixed in formalin for histopathology and snap frozen for protein extraction.

Measurement of prostate size

Prostate tissues from 6 month-old $APT_{121};Mdm2^{+/+}$ and $APT_{121};Mdm2^{C305F/C305F}$ mice as well as from their $Mdm2^{+/+}$ and $Mdm2^{C305F/C305F}$ littermate controls were excised, photographed, and weighed. All procedures involving mice were done according to a protocol approved by the University of North Carolina Institutional Animal Care and Use Committee.

Histopathology

Prostate tissues from $APT_{121};Mdm2^{+/+}$ and $APT_{121};Mdm2^{C305F/C305F}$ mice as well as from their $Mdm2^{+/+}$ and $Mdm2^{C305F/C305F}$ non-tumorigenic littermate controls, were fixed overnight in 10% phosphate-buffered formalin and then transferred to 70% ethanol. Samples were sent to the UNC Histology Core Facility for paraffin embedding. Paraffin blocks were sectioned at 5-μm intervals for successive layers and stained with hematoxylin (Sigma-Aldrich, St. Louis, MO) and eosin for histopathology examination.

Apoptosis analysis

Apoptosis levels of mouse prostate sections were assessed by the terminal deoxynucleotidyl transferase–mediated dUTP-biotin nick end labeling (TUNEL) assay (ApopTaq Peroxidease in situ Kit, Millipore, Temecula, CA). A ratio of TUNEL-positive stained cells to total cells counted was calculated. Statistical significance in differences in apoptosis levels between mice with different genotypes was evaluated by Student's t test ($P < 0.05$ was considered significant).

Proliferation analysis

Ki67 immunohistochemical staining of mouse prostate samples was used to detect proliferating cells. Antigen retrieval for antibody on formalin-fixed paraffin sections was done by boiling paraffin samples in citrate buffer (pH 6.0) for 15 min. Endogenous peroxidase

activity was quenched by incubation in 3% H_2O_2 in methanol for 10 minutes. Antibody detection was done by using purified mouse anti-human Ki67 primary antibody (BD Pharmigen, San Diego, CA) and biotin-conjugated anti-mouse secondary antibody (Vector Laboratories, Burlingame, CA). An avidin-biotin-peroxidase kit (Vectastain Elite, Vector Laboratories) with diaminobenzidine was used as a chromogen. A ratio of positive stained cells to total cells was calculated. Statistical significance in differences in proliferation levels between mice with different genotypes was evaluated by Student's t test ($P < 0.05$ was considered significant).

Culture of cells

Mouse keratinocyte cell lines and low-calcium culture media were provided by Dr. Marcelo Rodriguez-Puebla at North Carolina State University. MEF cells were isolated on embryonic day 13.5 (E 13.5) and cultured in DMEM (GIBCO, Carlsbad, CA) supplemented with 10% fetal bovine serum (GIBCO) and penicillin-streptomycin (GIBCO).

Retroviral infection of MEF cells

293 QBT cells (94) were transfected with plasmids: pVPack-Eco (viral coat protein plasmid for infecting mouse and rat cells), pVPack-Gag-Pol (viral protein plasmid) and pBabe or pBabe-H-Ras12V. Fugene HD kit was utilized for transfections, following manufacturer's instructions (Roche diagnostics, Indianapolis, IN). Virus-containing medium from 293 QBT cells was filtered through a 0.45 µm syringe-tip filter and mixed with fresh medium at the ratio of 1:1. Polybrene was added to the mixed medium to a final concentration of 6 µg/ml. The medium from primary mouse embryo fibroblasts (MEF) cells was removed and replaced with virus-containing medium. MEF cells were infected with a retrovirus derived from pBabe-puro-H-Ras12V or empty vector as a control, and stable polyclonal populations were selected by puromycin resistance.

Protein detection

Prostate tissues from $APT_{121};Mdm2^{+/+}$ and $APT_{121};Mdm2^{C305F/C305F}$ as well as from their $Mdm2^{+/+}$ and $Mdm2^{C305F/C305F}$ non-tumorigenic littermate controls were homogenized on ice and lysed in 0.5% NP-40 lysis buffer. Cultured cells (mouse keratinocytes and MEFs) were also lysed in 0.5% NP-40 lysis buffer. Total cellular lysates were run on a 12.5% SDS-polyacrymide gel followed by immunoblotting using standard procedures. Mouse monoclonal anti-p53 (NCL-505, Novocastra Laboratories, Newcastle upon Tyne, England) and anti-actin (MAB1501, Chemicon International, Temecula, CA) antibodies were purchased commercially. Rabbit polyclonal antibodies to L5 and L11 were produced as previously described (62).

CHAPTER FOUR

Summary and Future Directions

Role of p53 in APT$_{121}$-initiated Prostate Cancer Model

Previous study showed that loss of one or two alleles of p53 greatly accelerates the onset and progression of adenocarcinoma initiated by APT$_{121}$ (18, 51). However, genome wide loss of p53 is known to cause tumors in a variety of systems, such as lymphomas and sarcomas, which makes efforts to study its role in a single tissue difficult and does not reflect the true nature of prostate cancer progression in humans. The previous comparisons of tumor latency and mouse lifespan upon p53 loss were all on germline knockout mutants. Therefore, it is necessary to re-evaluate these in the somatic mutation system.

In this study, we generated a better pre-clinical mouse model for prostate cancer, in which pRb family members and p53 are somatically deleted in prostate epithelial cells. Deletion of p53 does accelerate the adenocarcinoma induced by APT$_{121}$. p53 is intact in the stroma of $APT_{121};p53^{cf/f};PbCre$ mice, yet tumors from $APT_{121};p53^{cf/f};PbCre$ mice are comprised of a large component of stromal cells, the same phenotype was also observed in $APT_{121};p53+/-$ and $APT_{121};p53-/-$ mice in the previous study. In APT$_{121}$; p53+/- mice, loss of heterozygosity (LOH) of p53 in the stroma happens before LOH of p53 in the epithelial cells induced by expression of T$_{121}$ in the epithelia. It was hypothesized that there is a cell

non-autonomous signal between epithelia and stroma (51). However, lack of one functional

copy of the p53 allele in the stromal cells may also promote LOH of p53 in stroma in the

APT_{121}p53 +/- mice in a cell-autonomous manner. To test this possibility, in the current study

of *$APT_{121};p53^{cf/f};PbCre$* mice, p53 is only deleted in prostate epithelial cells while stromal

tumors still occurred. This confirmed that the stromal expansion observed in *$APT_{121};p53$-/-*

mice is caused by paracine signaling from epithelial cells *per ce*. However, the paracrine

signaling remains unknown. It is also unknown that whether p53 in the stroma is loss or not

due to selection pressure. One way to address this will be to use laser capture

microdissection.

? Rb$_f$ p53 -/- → ? Rb$_f$ p53 -/-

p53 +/+   p53 -/- or p53+/+?
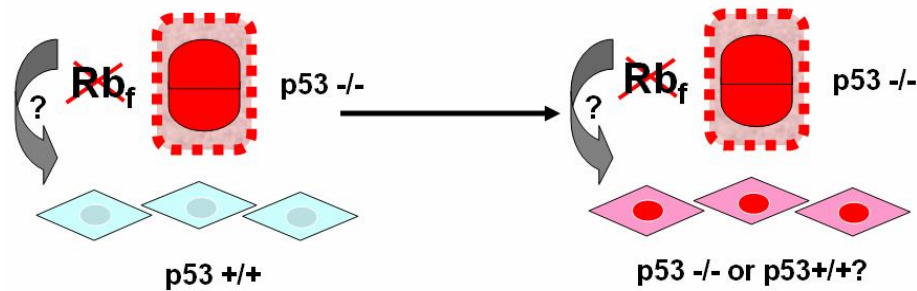
In addition, It has also been shown that carcinoma-associated fibroblasts (CAFs) can

accelerate the tumorigenesis in otherwise normal prostate epithelial cell layer (95). We would

like to explore whether neoplastic or normal epithelial cells progress to more severe states

through the influence of the supporting stromal cell layer. A useful system to study the

mesenchymal-epithelial interactions is the tissue recombination procedure developed by

Cunha and Lung (96). Briefly, mouse urogenital sinus mesenchyme (UGM) will be prepared

from 16-day embryonic fetuses of pregnant APT_{121} (C57BL/6) that will be crossed to p53KO^{+/-}

(C57BL/6) male. The possible genotypes of the pups are: wild-type (WT), APT_{121},

APT$_{121}$;p53KO$^{+/-}$ and p53KO$^{+/-}$. Separation of urogenital sinus mesenchyma (UGM) will be dissected from urogenital sinuses as previously described (97). The adult bladder urothelium mice will be separated from the stroma. Epithelial tissue fragments will then be recombined with UGM in neutralized type I rat tail collagen gels as previously described (98). Tissue recombinants will be grafted beneath the renal capsule of adult homozygous Rag1-/- male mice which are immune deficient due to lack of matured T and B cells. Mice will be euthanized and the grafts harvested. Using this system, it will be possible to determine whether cancer-associated fibroblasts can stimulate the tumor progression of nearby epithelial cells.

Our study confirmed that loss of p53 synergizes with loss of Rb to promote prostate tumorigenesis. However, it is unclear what downstream targets are disrupted by loss of p53 in this prostate cancer model. mRNA microarray can be done to search for potential downstream genes by comparing APT$_{121}$;p53$^{cf/f}$;Pb-Cre tumors with APT$_{121}$ tumors. Agilent mouse 4X44K Whole Mouse Genome Oligo Microarray Kit will be used. Real-time RT-PCR will be used to confirm gene expression difference. Western-blot will be done on prostate lysates to examine the protein expression of the whole prostate. Tissue microarrays (also TMAs) will also be done to immunodetect protein changes *in situ*.

Loss of p53 often induces genome instability. To see whether this contributes to the tumor progression in our APT$_{121}$ prostate model, we will measure the gene copy variation by CGH arrays (comparative genomic hybridization arrays). 5 months old is close to the terminal stage of for APT$_{121}$;p53$^{cf/f}$;Pb-Cre mice. Additional gene deletions may be accumulated due to

of tumor selection. Mouse Genomic CGH 4X44K arrays will be used on APT_{121};$p53^{cf/f}$;Pb-Cre

prostates of 5 months old to analyze copy number changes (gains/losses) caused by

prolonged loss of p53 and Rb.

Tumors harboring p53 mutations are often more vascularized and correlate with poor

prognosis for treatment (99). The significance of angiogenesis in prostate cancer is well

established. Many studies have demonstrated its direct correlation with Gleason score, tumor

stage, progression, metastasis and survival (100-102). From data mentioned above, it is

obvious that tumors from *APT_{121}; $p53^{cf/f}$; Pb-Cre* mice are more vascularized than those from

APT_{121} mice. To compare vasularization between *APT_{121}* and *APT_{121}; $p53^{cf/f}$; Pb-Cre* prostates

immnodetection of CD31will be used to visualize vessel structure in our tumor samples.

CD31 is also known as PECAM-1 (Platelet Endothelial Cell Adhesion Molecule-1).

CD31-mediated endothelial cell-cell interactions are involved in angiogenesis. In addition, we

will establish a collaboration with Dr. Paul Dayton at UNC to use his ultrasonic sound imaging

system and targeted microbubble contrast agents as a non-invasive tool to image vessels in

live murine prostate.

RP-Mdm2-p53 Pathway in Signaling Oncogenic Stress

Previous study showed that disruption of RP-Mdm2 binding accelerates B cell lymphoma.

This was the first time that RP-Mdm2-p53 signaling has been proved as a novel barrier in

response to oncogenic stress and leads us to question whether this signaling can play a

general in tumor suppression. To investigate this idea, we used a mouse model of prostate

cancer, APT$_{121}$, in which pRb and its family are inhibited. Our data demonstrated that

disruption of RP-Mdm2 binding does not accelerate the prostate cancer. Instead, deletion of

p19Arf greatly accelerates epithelial tumors and induces a unique stromal phenotype of

APT$_{121}$ prostate cancer as observed previously in p53-deficient background. Besides

investigating tumors induced by inactivation of pRb, we also examined the function of

RP-Mdm2-p53 in response to activation of Ras. Compared with *Mdm2$^{+/+}$* MEFs,

Mdm2$^{C305F/C305F}$ MEFs maintain a normal and comparable p53 response when Ras is

constitutively activate.
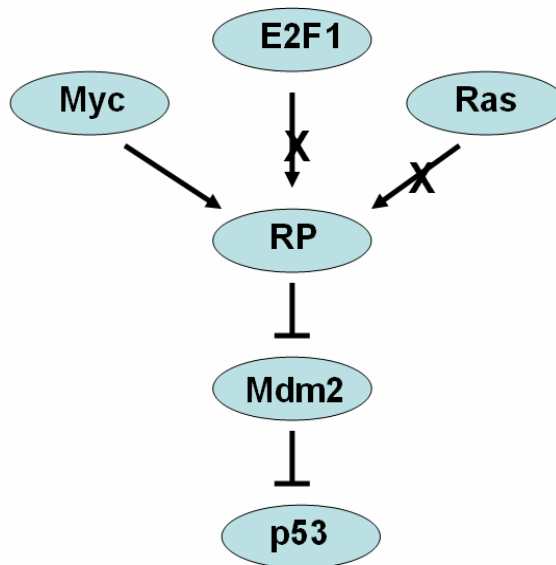
The reason why RP-Mdm2-p53 plays a critical role in Myc induced B cell lymphomas but

not in tumors induced by pRb inactivation is probably due to the lack of ribosomal stress in the

latter one. Consistent with this concept, Ras activation does not upregulate ribosomal proteins

either, and therefore, p53 signaling is intact regardless of the integrity of RP-Mdm2-p53

pathway. However, it is unknown whether this can be a rule to apply on all oncogenes, and consequently to determine if RP-Mdm2-p53 signaling is required or not for tumor suppression. One way to address this is to introduce a large panel of oncogenes individually into Mdm2$^{+/+}$ and Mdm2$^{C305F/C305F}$ MEFs and then categorize them into two groups: those that upregulate ribosomal proteins and those do not upregulate ribosomal proteins. If the p53 response is attenuated in the former group while it remains intact in the latter group, we can conclude that RP-Mdm2-p53 is required only when a certain oncogene induces ribosomal stress, such as overexpression of ribosomal proteins. If not, the alternative explanation may be that functional RP-Mdm2-p53 signaling only suppresses tumor types that increase quickly in their volume, such as lymphoma, yet this signaling does not inhibit tumor types that take a long time to grow, such as prostate cancer.

Another issue we ponder on is why *Mdm2$^{C305F/C305F}$* mice exhibit a smaller prostate than wild-type mice. *Mdm2$^{C305F/C305F}$* male mice are slightly smaller than their wild-type counterparts in the body size too, though the difference is not statistically significant (data not shown). Recently p53 has been reported to promote cell survival through induction of *TIGAR* (*T*P53-*i*nduced *g*lycolysis and *a*poptosis *r*egulator) (93). It is possible that *Mdm2$^{C305F/C305F}$* mice have slightly lower level of p53 than is needed for normal cell growth and survival, and therefore, mice are slightly smaller in body size as well as some organs. To investigate this possibility, endogenous p53 level from tissues of Mdm2$^{+/+}$ and Mdm2$^{C305F/C305F}$ mice need to be determined.

p53 has been recognized as a tumor suppressor gene to control cell proliferation and

growth for a long time. However, p53 is conserved across species and even zebrafish has p53 protein. It is apparent however that zebrafish does not have tumors and therefore, what is the fundamental function of p53? It is likely that p53 also functions to protect organs or cells from daily stress, for instance metabolic stress. Given that in the Mdm2^{C305F} mouse model, ribosomal stress signaling to p53 is disrupted by point mutation of Mdm2, this mouse can be a good model to study the role of p53 in response to metabolic stress. Studies designed to treat mice under metabolic stress, such as fasting, are in process.

In summary, RP-Mdm2-p53 has been shown as a novel signaling pathway specifically in response to Myc induced lymphoma. Beyond that, more can be learned about the roles of this signaling pathway in response to daily stress by using the Mdm2^{C305F} mouse model.

REFERENCES

1. SEER Ns. NCI's SEER Cancer Statistics Review 1975-2005.

2. Walsh PC. Heterogeneity of genetic alterations in prostate cancer: evidence of the complex nature of the disease. J Urol. 2002;168(4 Pt 1):1635-6.

3. Bookstein R, Rio P, Madreperla SA, Hong F, Allred C, Grizzle WE, et al. Promoter deletion and loss of retinoblastoma gene expression in human prostate carcinoma. Proc Natl Acad Sci U S A. 1990;87(19):7762-6. PMCID: 54828.

4. Henke RP, Kruger E, Ayhan N, Hubner D, Hammerer P, Huland H. Immunohistochemical detection of p53 protein in human prostatic cancer. J Urol. 1994;152(4):1297-301.

5. Dyson N. pRB, p107 and the regulation of the E2F transcription factor. JCell Sci. 1994.

6. Brehm A, Miska EA, McCance DJ, Reid JL, Bannister AJ, Kouzarides T. Retinoblastoma protein recruits histone deacetylase to repress transcription. Nature. 1998;391(6667):597-601.

7. Magnaghi-Jaulin L, Groisman R, Naguibneva I, Robin P, Lorain S, Le Villain JP, et al. Retinoblastoma protein represses transcription by recruiting a histone deacetylase. Nature. 1998;391(6667):601-5.

8. Stiegler P, De Luca A, Bagella L, Giordano A. The COOH-terminal region of pRb2/p130 binds to histone deacetylase 1 (HDAC1), enhancing transcriptional repression of the E2F-dependent cyclin A promoter. Cancer Res. 1998;58(22):5049-52.

9. Li C, Larsson C, Futreal A, Lancaster J, Phelan C, Aspenblad U, et al. Identification of two distinct deleted regions on chromosome 13 in prostate cancer. Oncogene. 1998;16(4):481-7.

10. Melamed J, Einhorn JM, Ittmann MM. Allelic loss on chromosome 13q in human prostate carcinoma. Clin Cancer Res. 1997;3(10):1867-72.

11. Tricoli JV, Gumerlock PH, Yao JL, Chi SG, D'Souza SA, Nestok BR, et al. Alterations of the retinoblastoma gene in human prostate adenocarcinoma. Genes Chromosomes Cancer. 1996;15(2):108-14.

12. Jacks T, Fazeli A, Schmitt EM, Bronson RT, Goodell MA, Weinberg RA. Effects of an Rb mutation in the mouse. Nature. 1992;359(6393):295-300.

13. Williams BO, Remington L, Albert DM, Mukai S, Bronson RT, Jacks T. Cooperative tumorigenic effects of germline mutations in Rb and p53. Nat Genet. 1994;7(4):480-4.

14. Hu NP, Gutsmann A, Herbert DC, Bradley A, Lee WH, Lee EYHP. Heterozygous Rb-1(Delta-20)/+ Mice Are Predisposed to Tumors of the Pituitary-Gland with a Nearly Complete Penetrance. Oncogene. 1994;9(4):1021-7.

15. Maandag ECR, Vandervalk M, Vlaar M, Feltkamp C, Obrien J, Vanroon M, et al. Developmental Rescue of an Embryonic-Lethal Mutation in the Retinoblastoma Gene in Chimeric Mice. Embo J. 1994;13(18):4260-8.

16. Maddison LA, Sutherland BW, Barrios RJ, Greenberg NM. Conditional deletion of Rb causes early stage prostate cancer. Cancer Research. 2004;64(17):6018-25.

17. Marino S, Vooijs M, van Der Gulden H, Jonkers J, Berns A. Induction of medulloblastomas in p53-null mutant mice by somatic inactivation of Rb in the external granular layer cells of the cerebellum. Genes Dev. 2000;14(8):994-1004. PMCID: 316543.

18. Hill R, Song Y, Cardiff RD, Van Dyke T. Heterogeneous tumor evolution initiated by loss of pRb function in a preclinical prostate cancer model. Cancer Res. 2005;65(22):10243-54.

19. Christophorou MA, Martin-Zanca D, Soucek L, Lawlor ER, Brown-Swigart L, Verschuren EW, et al. Temporal dissection of p53 function in vitro and in vivo. Nat Genet. 2005;37(7):718-26.

20. Vater CA, Bartle LM, Dionne CA, Littlewood TD, Goldmacher VS. Induction of apoptosis by tamoxifen-activation of a p53-estrogen receptor fusion protein expressed in E1A and T24 H-ras transformed p53(-/-) mouse embryo fibroblasts. Oncogene. 1996;13(4):739-48.

21. Vogelstein B, Lane D, Levine AJ. Surfing the p53 network. Nature. 2000;408(6810):307-10.

22. Picksley SM, Lane DP. The p53-mdm2 autoregulatory feedback loop: a paradigm for the regulation of growth control by p53? Bioessays. 1993;15(10):689-90.

23. Hollstein M, Sidransky D, Vogelstein B, Harris CC. p53 mutations in human cancers. Science. 1991;253(5015):49-53.

24. Leach FS, Tokino T, Meltzer P, Burrell M, Oliner JD, Smith S, et al. p53 Mutation and MDM2 amplification in human soft tissue sarcomas. Cancer Res. 1993;53(10 Suppl):2231-4.

25. Perry RP. Balanced production of ribosomal proteins. Gene. 2007;401(1-2):1-3.

26. Sun XX, Dai MS, Lu H. Mycophenolic acid activation of p53 requires ribosomal proteins l5 and l11. Journal of Biological Chemistry. 2008;283(18):12387-92.

27. Dai MS, Lu H. Inhibition of MDM2-mediated p53 ubiquitination and degradation by ribosomal protein L5 (vol 279, 44475, 2004). Journal of Biological Chemistry. 2004;279(50):-.

28. Gilkes DM, Chen LH, Chen JD. MDMX regulation of p53 response to ribosomal stress. Embo J. 2006;25(23):5614-25.

29. Bhat KP, Itahana K, Jin AW, Zhang YP. Essential role of ribosomal protein L11 in mediating growth inhibition-induced p53 activation. Embo J. 2004;23(12):2402-12.

30. Dai MS, Sun XX, Lu H. Aberrant expression of nucleostemin activates p53 and induces cell cycle arrest via inhibition of MDM2. Molecular and Cellular Biology. 2008;28(13):4365-76.

31. Lohrum MAE, Ludwig RL, Kubbutat MHG, Hanlon M, Vousden KH. Regulation of HDM2 activity by the ribosomal protein L11. Cancer Cell. 2003;3(6):577-87.

32. Zhang YP, Wolf GW, Bhat K, Jin A, Allio T, Burkhart WA, et al. Ribosomal protein L11 negatively regulates oncoprotein MDM2 and mediates a p53-dependent ribosomal-stress checkpoint pathway. Molecular and Cellular Biology. 2003;23(23):8902-12.

33. Jin A, Itahana K, O'Keefe K, Zhang Y. Inhibition of HDM2 and activation of p53 by ribosomal protein L23. Molecular and Cellular Biology. 2004;24(17):7669-80.

34. Dai MS, Lu H. Inhibition of MDM2-mediated p53 ubiquitination and degradation by ribosomal protein L5. Journal of Biological Chemistry. 2004;279(43):44475-82.

35. Chen D, Zhang Z, Li M, Wang W, Li Y, Rayburn ER, et al. Ribosomal protein S7 as a novel modulator of p53-MDM2 interaction: binding to MDM2, stabilization of p53 protein, and activation of p53 function. Oncogene. 2007;26(35):5029-37.

36. Zhu Y, Poyurovsky MV, Li YC, Biderman L, Stahl J, Jacq X, et al. Ribosomal Protein S7 Is Both a Regulator and a Substrate of MDM2. Molecular Cell. 2009;35(3):316-26.

37. Ofir-Rosenfeld Y, Boggs K, Michael D, Kastan MB, Oren M. Mdm2 Regulates p53 mRNA Translation through Inhibitory Interactions with Ribosomal Protein L26. Molecular Cell. 2008;32(2):180-9.

38. Zhang Y, Lu H. Signaling to p53: ribosomal proteins find their way. Cancer Cell. 2009;16(5):369-77.

39. Lindstrom MS, Jin AW, Deisenroth C, Wolf GW, Zhang YP. Cancer-associated mutations in the MDM2 zinc finger domain disrupt ribosomal protein interaction and attenuate MDM2-induced p53 degradation. Molecular and Cellular Biology. 2007;27(3):1056-68.

40. Macias E, Jin A, Deisenroth C, Bhat K, Mao H, Lindstrom MS, et al. An ARF-independent c-MYC-activated tumor suppression pathway mediated by ribosomal protein-Mdm2 Interaction. Cancer Cell. 2010;18(3):231-43.

41. Alitalo K, Koskinen P, Makela TP, Saksela K, Sistonen L, Winqvist R. Myc-Oncogenes - Activation and Amplification. Biochimica Et Biophysica Acta. 1987;907(1):1-32.

42. Adams JM, Harris AW, Pinkert CA, Corcoran LM, Alexander WS, Cory S, et al. The C-Myc Oncogene Driven by Immunoglobulin Enhancers Induces Lymphoid Malignancy in Transgenic Mice. Nature. 1985;318(6046):533-8.

43. Dai MS, Lu H. Crosstalk Between c-Myc and Ribosome in Ribosomal Biogenesis and Cancer. Journal of Cellular Biochemistry. 2008;105(3):670-7.

44. Eischen CM, Weber JD, Roussel MF, Sherr CJ, Cleveland JL. Disruption of the ARF-Mdm2-p53 tumor suppressor pathway in Myc-induced lymphomagenesis. Gene Dev. 1999;13(20):2658-69.

45. Navone NM, Troncoso P, Pisters LL, Goodrow TL, Palmer JL, Nichols WW, et al. p53 protein accumulation and gene mutation in the progression of human prostate carcinoma. J Natl Cancer Inst. 1993;85(20):1657-69.

46. Phillips SMA, Barton CM, Lee SJ, Morton DG, Wallace DMA, Lemoine NR, et al. Loss of the Retinoblastoma Susceptibility Gene (Rb1) Is a Frequent and Early Event in Prostatic Tumorigenesis. Brit J Cancer. 1994;70(6):1252-7.

47. Heidenberg HB, Sesterhenn IA, Gaddipati JP, Weghorst CM, Buzard GS, Moul JW, et al. Alteration of the Tumor-Suppressor Gene P53 in a High Fraction of Hormone-Refractory Prostate-Cancer. Journal of Urology. 1995;154(2):414-21.

48. Wu XT, Wu J, Huang JP, Powell WC, Zhang JF, Matusik RJ, et al. Generation of a prostate epithelial cell-specific Cre transgenic mouse model for tissue-specific gene ablation. Mech Develop. 2001;101(1-2):61-9.

49. Zhou Z, Flesken-Nikitin A, Corney DC, Wang W, Goodrich DW, Roy-Burman P, et al. Synergy of p53 and Rb deficiency in a conditional mouse model for metastatic prostate cancer. Cancer Res. 2006;66(16):7889-98.

50. Zhou Z, Flesken-Nikitin A, Nikitin AY. Prostate cancer associated with p53 and Rb deficiency arises from the stem/progenitor cell-enriched proximal region of prostatic ducts. Cancer Res. 2007;67(12):5683-90.

51. Hill R, Song Y, Cardiff RD, Van Dyke T. Selective evolution of stromal mesenchyme with p53 loss in response to epithelial tumorigenesis. Cell. 2005;123(6):1001-11.

52. Jonkers J, Berns A. Conditional mouse models of sporadic cancer. Nat Rev Cancer. 2002;2(4):251-65.

53. Chen Z, Trotman LC, Shaffer D, Lin HK, Dotan ZA, Niki M, et al. Crucial role of p53-dependent cellular senescence in suppression of Pten-deficient tumorigenesis. Nature. 2005;436(7051):725-30. PMCID: 1939938.

54. Gaudin PB, Rosai J, Epstein JI. Sarcomas and related proliferative lesions of specialized prostatic stroma: a clinicopathologic study of 22 cases. Am J Surg Pathol. 1998;22(2):148-62.

55. Hossain D, Meiers I, Qian J, MacLennan GT, Bostwick DG. Prostatic stromal hyperplasia with atypia: follow-up study of 18 cases. Arch Pathol Lab Med. 2008;132(11):1729-33.

56. Herawi M, Epstein JI. Specialized stromal tumors of the prostate: a clinicopathologic study of 50 cases. Am J Surg Pathol. 2006;30(6):694-704.

57. Chiaverotti T, Couto SS, Donjacour A, Mao JH, Nagase H, Cardiff RD, et al. Dissociation of epithelial and neuroendocrine carcinoma lineages in the transgenic adenocarcinoma of mouse prostate model of prostate cancer. Am J Pathol. 2008;172(1):236-46. PMCID: 2189611.

58. Howlader N NA, Krapcho M, Neyman N, Aminou R, Waldron W, Altekruse SF, Kosary CL, Ruhl J, Tatalovich Z, Cho H, Mariotto A, Eisner MP, Lewis DR, Chen HS, Feuer EJ, Cronin KA, Edwards BK. SEER Cancer Statistics Review 1975-2008. SEER. 2011.

59. Lohrum MA, Ludwig RL, Kubbutat MH, Hanlon M, Vousden KH. Regulation of HDM2 activity by the ribosomal protein L11. Cancer Cell. 2003;3(6):577-87.
60. Dai MS, Zeng SX, Jin YT, Sun XX, David L, Lu H. Ribosomal protein L23 activates p53 by inhibiting MDM2 function in response to ribosomal perturbation but not to translation

inhibition. Molecular and Cellular Biology. 2004;24(17):7654-68.

61. Zhang YP, Lu H. Signaling to p53: Ribosomal Proteins Find Their Way. Cancer Cell. 2009;16(5):369-77.

62. Lindstrom MS, Jin A, Deisenroth C, White Wolf G, Zhang Y. Cancer-associated mutations in the MDM2 zinc finger domain disrupt ribosomal protein interaction and attenuate MDM2-induced p53 degradation. Mol Cell Biol. 2007;27(3):1056-68. PMCID: 1800693.

63. Arabi A, Wu SQ, Ridderstrale K, Bierhoff H, Shiue C, Fatyol K, et al. c-Myc associates with ribosomal DNA and activates RNA polymerase I transcription. Nat Cell Biol. 2005;7(3):303-10.

64. Grewal SS, Li L, Orian A, Eisenman RN, Edgar BA. Myc-dependent regulation of ribosomal RNA synthesis during Drosophila development. Nat Cell Biol. 2005;7(3):295-U109.

65. Boon K, Caron HN, van Asperen R, Valentijn L, Hermus MC, van Sluis P, et al. N-myc enhances the expression of a large set of genes functioning in ribosome biogenesis and protein synthesis. Embo J. 2001;20(6):1383-93.

66. Coller HA, Grandori C, Tamayo P, Colbert T, Lander ES, Eisenman RN, et al. Expression analysis with oligonucleotide microarrays reveals that MYC regulates genes involved in growth, cell cycle, signaling, and adhesion. Proceedings of the National Academy of Sciences of the United States of America. 2000;97(7):3260-5.

67. Guo QM, Malek RL, Kim S, Chiao C, He M, Ruffy M, et al. Identification of c-Myc responsive genes using rat cDNA microarray. Cancer Research. 2000;60(21):5922-8.

68. Menssen A, Hermeking H. Characterization of the c-MYC-regulated transcriptome by SAGE: Identification and analysis of c-MYC target genes. Proceedings of the National Academy of Sciences of the United States of America. 2002;99(9):6274-9.

69. Gomez-Roman N, Grandori C, Eisenman RN, White RJ. Direct activation of RNA polymerase III transcription by c-Myc. Nature. 2003;421(6920):290-4.

70. Kamijo T, Weber JD, Zambetti G, Zindy F, Roussel MF, Sherr CJ. Functional and physical interactions of the ARF tumor suppressor with p53 and Mdm2. Proc Natl Acad Sci U S A. 1998;95(14):8292-7. PMCID: 20969.

71. Zhang YP, Xiong Y, Yarbrough WG. ARF promotes MDM2 degradation and stabilizes p53: ARF-INK4a locus deletion impairs both the Rb and p53 tumor suppression pathways. Cell. 1998;92(6):725-34.

72. Pomerantz J, Schreiber-Agus N, Liegeois NJ, Silverman A, Alland L, Chin L, et al. The Ink4a tumor suppressor gene product, p19Arf, interacts with MDM2 and neutralizes MDM2's inhibition of p53. Cell. 1998;92(6):713-23.

73. Stott FJ, Bates S, James MC, McConnell BB, Starborg M, Brookes S, et al. The alternative product from the human CDKN2A locus, p14(ARF), participates in a regulatory feedback loop with p53 and MDM2. Embo J. 1998;17(17):5001-14. PMCID: 1170828.

74. Bates S, Phillips AC, Clark PA, Stott F, Peters G, Ludwig RL, et al. p14ARF links the tumour suppressors RB and p53. Nature. 1998;395(6698):124-5.

75. Kamijo T, Zindy F, Roussel MF, Quelle DE, Downing JR, Ashmun RA, et al. Tumor suppression at the mouse INK4a locus mediated by the alternative reading frame product p19ARF. Cell. 1997;91(5):649-59.

76. Lin AW, Lowe SW. Oncogenic ras activates the ARF-p53 pathway to suppress epithelial cell transformation. Proc Natl Acad Sci U S A. 2001;98(9):5025-30. PMCID: 33157.

77. Tolbert D, Lu XD, Yin CY, Tantama M, Van Dyke T. p19(ARF) is dispensable for oncogenic stress-induced p53-mediated apoptosis and tumor suppression in vivo. Molecular and Cellular Biology. 2002;22(1):370-7.

78. Roper E, Weinberg W, Watt FM, Land H. p19ARF-independent induction of p53 and cell cycle arrest by Raf in murine keratinocytes. EMBO Rep. 2001;2(2):145-50. PMCID: 1083816.

79. Ayrault O, Andrique L, Seite P. Involvement of the transcriptional factor E2F1 in the regulation of the rRNA promoter. Experimental Cell Research. 2006;312(7):1185-93.

80. Jorgensen P, Rupes I, Sharom JR, Schneper L, Broach JR, Tyers M. A dynamic transcriptional network communicates growth potential to ribosome synthesis and critical cell size. Genes Dev. 2004;18(20):2491-505. PMCID: 529537.

81. Fingar DC, Richardson CJ, Tee AR, Cheatham L, Tsou C, Blenis J. mTOR controls cell cycle progression through its cell growth effectors S6K1 and 4E-BP1/eukaryotic translation initiation factor 4E. Molecular and Cellular Biology. 2004;24(1):200-16.

82. Dyson N. pRB, p107 and the regulation of the E2F transcription factor. J Cell Sci Suppl. 1994;18:81-7.

83. Zhou ZX, Flesken-Nikitin A, Corney DC, Wang W, Goodrich DW, Roy-Burman P, et al.

Synergy of p53 and Rb deficiency in a conditional mouse model for metastatic prostate cancer. Cancer Research. 2006;66(16):7889-98.

84. Palmero I, Pantoja C, Serrano M. p19ARF links the tumour suppressor p53 to Ras. Nature. 1998;395(6698):125-6.

85. Zindy F, Eischen CM, Randle DH, Kamijo T, Cleveland JL, Sherr CJ, et al. Myc signaling via the ARF tumor suppressor regulates p53-dependent apoptosis and immortalization. Genes Dev. 1998;12(15):2424-33. PMCID: 317045.

86. Bookstein R, Macgrogan D, Hilsenbeck SG, Sharkey F, Allred DC. P53 Is Mutated in a Subset of Advanced-Stage Prostate Cancers. Cancer Research. 1993;53(14):3369-73.

87. Heidenberg HB, Sesterhenn IA, Gaddipati JP, Weghorst CM, Buzard GS, Moul JW, et al. Alteration of the tumor suppressor gene p53 in a high fraction of hormone refractory prostate cancer. J Urol. 1995;154(2 Pt 1):414-21.

88. Downward J. Targeting ras signalling pathways in cancer therapy. Nature Reviews Cancer. 2003;3(1):11-22.

89. Fingar DC, Blenis J. Target of rapamycin (TOR): an integrator of nutrient and growth factor signals and coordinator of cell growth and cell cycle progression. Oncogene. 2004;23(18):3151-71.

90. Yuspa SH, Kulesz-Martin M, Ben T, Hennings H. Transformation of epidermal cells in culture. J Invest Dermatol. 1983;81(1 Suppl):162s-8s.

91. Conti CJ, Fries JW, Viaje A, Miller DR, Morris R, Slaga TJ. In vivo behavior of murine epidermal cell lines derived from initiated and noninitiated skin. Cancer Res. 1988;48(2):435-9.

92. Bassi DE, Zhang J, Cenna J, Litwin S, Cukierman E, Klein-Szanto AJ. Proprotein convertase inhibition results in decreased skin cell proliferation, tumorigenesis, and metastasis. Neoplasia. 2010;12(7):516-26. PMCID: 2907578.

93. Bensaad K, Tsuruta A, Selak MA, Vidal MN, Nakano K, Bartrons R, et al. TIGAR, a p53-inducible regulator of glycolysis and apoptosis. Cell. 2006;126(1):107-20.

94. Deisenroth C, Thorner AR, Enomoto T, Perou CM, Zhang YP. Mitochondrial HEP27 Is a c-Myb Target Gene That Inhibits Mdm2 and Stabilizes p53. Molecular and Cellular Biology. 2010;30(16):3981-93.

95. Cunha GR, Hayward SW, Wang YZ, Ricke WA. Role of the stromal microenvironment in carcinogenesis of the prostate. Int J Cancer. 2003;107(1):1-10.

96. Cunha GR, Lung B. The possible influence of temporal factors in androgenic responsiveness of urogenital tissue recombinants from wild-type and androgen-insensitive (Tfm) mice. J Exp Zool. 1978;205(2):181-93.

97. Cunha GR DA. Mesenchymal-epithelial interactions: technical considerations. 1987.

98. Hayward SW, Haughney PC, Rosen MA, Greulich KM, Weier HUG, Dahiya R, et al. Interactions between adult human prostatic epithelium and rat urogenital sinus mesenchyme in a tissue recombination model. Differentiation. 1998;63(3):131-40.

99. Teodoro JG, Evans SK, Green MR. Inhibition of tumor angiogenesis by p53: a new role for the guardian of the genome. J Mol Med. 2007;85(11):1175-86.

100.   Borre M, Offersen BV, Nerstrom B, Overgaard J. Microvessel density predicts survival in prostate cancer patients subjected to watchful waiting. Br J Cancer. 1998;78(7):940-4.

101.   Bono AV, Celato N, Cova V, Salvadore M, Chinetti S, Novario R. Microvessel density in prostate carcinoma. Prostate Cancer Prostatic Dis. 2002;5(2):123-7.

102.   Strohmeyer D, Strauss F, Rossing C, Roberts C, Kaufmann O, Bartsch G, et al. Expression of bFGF, VEGF and c-met and their correlation with microvessel density and progression in prostate carcinoma. Anticancer Res. 2004;24(3a):1797-804.